

Oxford Preprint: OUTP-97-20P  
May 1997

# Leptonic Decays of Heavy Quarks on the Lattice

**Hartmut Wittig**

Theoretical Physics, University of Oxford,  
1 Keble Road, Oxford OX1 3NP, UK

## **Abstract**

The status of lattice calculations of heavy-light decay constants and of the  $B$  parameter  $B_B$  is reviewed. After describing the lattice approach to heavy quark systems, the main results are discussed, with special emphasis on the systematic errors in present lattice calculations. A detailed analysis of the continuum limit for decay constants is performed. The implications of lattice results on studies of CP violation in the Standard Model are discussed.

(Submitted to International Journal of Modern Physics A)



## LEPTONIC DECAYS OF HEAVY QUARKS ON THE LATTICE

HARTMUT WITTIG

*Theoretical Physics, University of Oxford, 1 Keble Road  
Oxford OX1 3NP, UK*

Received (received date)

Revised (revised date)

The status of lattice calculations of heavy-light decay constants and of the  $B$  parameter  $B_B$  is reviewed. After describing the lattice approach to heavy quark systems, the main results are discussed, with special emphasis on the systematic errors in present lattice calculations. A detailed analysis of the continuum limit for decay constants is performed. The implications of lattice results on studies of CP violation in the Standard Model are discussed.

### 1. Introduction

Heavy quark systems have attracted a lot of interest in the past decade. Theoretical and experimental investigations of weak decays of heavy quark systems offer the main sources of information on the phenomenon of CP violation in the Standard Model. Our understanding of CP violation is directly related to the knowledge of the elements of the Cabibbo-Kobayashi-Maskawa (CKM) matrix, which describes the pattern of quark mixing in flavour-changing charged current interactions. Within the framework of the Standard Model the CKM matrix is unitary, and, provided that one can determine its elements with high enough precision, any deviation from unitarity would be interpreted as a hint of “new physics”. The theoretical treatment of weak decay amplitudes involving heavy quarks is, however, hampered by large uncertainties due to strong interactions. Since quarks are confined within hadrons, the exchange of soft gluons between them makes weak decay matrix elements intractable in perturbation theory. Therefore, other theoretical tools have to be applied in order to deal with the intrinsic non-perturbative nature of weak decays of hadronic systems, e.g. QCD sum rules<sup>1</sup> or lattice gauge theories<sup>2,3</sup>. Another formalism which can be applied specifically to heavy quark systems is provided by the Heavy Quark Symmetry and the Heavy Quark Effective Theory (HQET)<sup>4–12</sup>.

Lattice gauge theories offer the possibility of a systematic non-perturbative treatment of strong interaction effects in weak decay amplitudes. Indeed, Monte Carlo simulations of lattice QCD have made important contributions to our understanding of hadronic physics by providing non-perturbative, model-independent estimates for a number of quantities, which are relevant for the spectrum and weak decays of hadronic systems in general. An important ingredient in non-perturbative

studies of weak decays is the operator product expansion<sup>13</sup>. In general, a weak amplitude, which usually involves the product of two hadronic currents, can be written as a sum over local operators, viz.

$$\mathcal{A}(f \leftarrow i) = \sum_n C_n(\mu) \langle f | \hat{O}_n(\mu) | i \rangle. \quad (1)$$

Here,  $\mu$  is the renormalisation scale, and the Wilson coefficients  $C_n(\mu)$ , which contain the short-distance physics, are independent of the initial and final states and can be computed in perturbation theory for  $\mu \gg \Lambda_{\text{QCD}}$ . The matrix element  $\langle f | \hat{O}_n(\mu) | i \rangle$ , on the other hand, describes the long-distance physics, contains strong interaction contributions and must be calculated non-perturbatively, e.g. in a lattice simulation.

The rôle of lattice simulations in the analysis of weak matrix elements is two-fold. First, they serve to test QCD, as lattice data can be compared to experiment or to results obtained using HQET or QCD sum rules. Second, they can make predictions for yet unmeasured quantities like the decay constant  $f_B$ . In fact,  $f_B$  (or rather the combination  $f_B \sqrt{B_B}$ , where  $B_B$  is the  $B$  parameter relevant for  $B^0 - \bar{B}^0$  mixing) is the principal unknown quantity in the analysis of CP violation in the heavy quark sector. If lattice QCD is to have a serious impact on testing the consistency of the Standard Model, then it is clear that the control over systematic errors in the lattice approach is of paramount importance.

There exists by now a vast amount of literature on lattice results for heavy-light decay constants, which will be discussed in detail in this review, pointing out the differences between various calculations and assessing their inherent systematic errors. Another aim of this study is to combine as many lattice results as possible in a systematic fashion, and to provide the currently best estimate for  $f_B \sqrt{B_B}$  computed on the lattice. The present status of lattice calculations of  $B$  meson decay constants and  $B$  parameters can be summarised as follows

$$f_B = 172^{+27}_{-31} \text{ MeV}, \quad f_{B_s}/f_{B_d} = 1.14 \pm 0.08, \quad (2)$$

$$f_B \sqrt{\hat{B}_B} = 195^{+30}_{-40} \text{ MeV}, \quad \hat{B}_B = 1.3^{+2}_{-3}, \quad (3)$$

where  $\hat{B}_B$  is the renormalisation group invariant  $B$  parameter. In the following sections we will review lattice data from several groups and describe the derivation of the global results above.

An overview of the development of this area of lattice gauge theories can be gained by consulting various review talks in the proceedings of recent lattice conferences<sup>14–18</sup>. Other reviews and pedagogical introductions can be found in refs.<sup>19–26</sup>.

We begin this review in section 2 with a brief introduction to lattice QCD for the non-specialist and describe the lattice approach to heavy quark systems. In section 3 we discuss lattice results for heavy-light decay constants. A detailed, if somewhat technical analysis of the continuum limit is presented in subsection 3.4, which may be skipped if the reader is not so interested in the technical details.

Section 4 contains the discussion of lattice results for the  $B$  parameter  $B_B$ . The implications of our findings on the study of CP violation is presented in section 5. Finally, section 6 contains some concluding remarks. Two appendices are added, which present details of the matching between lattice matrix elements and their continuum counterparts, as well as a summary of lattice data in the light hadron sector.

## 2. Lattice Approach to Heavy Quark Systems

In this section we present the basic concepts of lattice QCD before various formulations of heavy quarks on the lattice are discussed in some detail. Furthermore, the relation between weak matrix elements on the lattice and their continuum counterparts is discussed, and at the end of this section we summarise the main systematic errors which affect lattice results for heavy quark physics.

### 2.1. Lattice QCD and numerical simulations

Since its original foundation by Wilson in 1974<sup>2,3</sup>, lattice QCD has developed into a mature area of research in elementary particle physics. In general, the lattice approach now forms an important part in the study of a large class of quantum field theories, ranging from scalar field theory to quantum gravity.

One important aspect in the study of lattice field theories is that they are suitable for numerical methods such as Monte Carlo simulations. Indeed, the biggest impact lattice QCD has had on phenomenology in the past decade has originated from large-scale numerical simulations. The strength of this approach is based on the fact that the lattice is currently the only known non-perturbative regulator of a quantum field theory which is systematically improvable.

In this subsection we will briefly discuss the basic features of the formulation and the implementation of lattice QCD in Monte Carlo simulations. For more detailed information, the reader is referred to several good textbooks<sup>27,28,29</sup>.

In order to be easily accessible to computer simulations, lattice QCD is usually formulated in euclidean space-time. For a finite system, the lattice size is  $L^3 \cdot T$ , where  $L^3$  is the spatial volume, and  $T$  is the extension of the lattice in the time direction. The lattice sites are separated by the lattice spacing  $a$ . It is easy to show that the lattice spacing acts as an UV cut-off. Present computers can handle lattices of typically  $16^4$  to  $48^4$  lattice sites. Thus, to be able to accommodate a hadron, the physical length of the lattice should not be smaller than about 1.5 fm. This implies that values of the lattice spacing in physical units must lie in the range of  $a = 0.1\text{--}0.05$  fm.

On the lattice, non-abelian gauge fields are represented by so-called *link variables*, which connect neighbouring sites. These link variables, which carry a Lorentz index  $\mu$ , are elements of the gauge group (here: SU(3)). Given a link variable  $U_\mu(x)$  emanating from site  $x$  in direction  $\mu = 1, \dots, 4$ , one can define a vector field  $A_\mu(x)$

as an element of the Lie algebra of the gauge group  $SU(3)$  via

$$e^{iaA_\mu(x)} \equiv U_\mu(x) \in SU(3). \quad (4)$$

The simplest lattice version of the action of a Yang-Mills theory is the Wilson plaquette action<sup>2</sup>

$$S_G[U] = \beta \sum_x \sum_{\mu < \nu} \left( 1 - \frac{1}{3} \text{Re Tr } P_{\mu\nu}(x) \right), \quad \beta = 6/g_0^2 \quad (5)$$

where  $P_{\mu\nu}(x) \equiv U_\mu(x)U_\nu(x + \hat{\mu})U_\mu^\dagger(x + \hat{\nu})U_\nu^\dagger(x)$  is the product of links around an elementary square of the lattice, the “plaquette”, and  $g_0$  is the bare gauge coupling. Here,  $\hat{\mu}$  denotes a vector in direction  $\mu$  of length  $a$ , such that  $x + \hat{\mu}$  is the neighbouring site of  $x$  in direction  $\mu$ . Using the definition of the field  $A_\mu(x)$  in eq. (4), one can show that for small lattice spacings, the term in  $S_G[U]$  reduces to the familiar expression  $-\frac{1}{g_0^2} \text{Tr } F_{\mu\nu}^2$ .

Quark and antiquark fields,  $\psi(x)$ ,  $\bar{\psi}(x)$  are associated with the lattice sites. Using the link variable  $U_\mu(x)$ , a possible definition of the covariant derivative is given by

$$D_\mu \psi(x) \equiv \frac{1}{a} \{ U_\mu(x) \psi(x + \hat{\mu}) - \psi(x) \} \quad (6)$$

$$\bar{\psi}(x) \overleftarrow{D}_\mu \equiv \frac{1}{a} \{ \bar{\psi}(x + \hat{\mu}) U_\mu^\dagger(x) - \bar{\psi}(x) \}. \quad (7)$$

In euclidean space-time, the Dirac matrices can be defined to satisfy

$$\{\gamma_\mu, \gamma_\nu\} = 2\delta_{\mu\nu}. \quad (8)$$

Now we are in a position to write down a latticised version of the QCD Lagrangian. It turns out, however, that the naïve lattice transcription of the fermionic part suffers from the notorious fermion doubling problem: in the case of a free Dirac particle it simply means that, in four dimensions of space-time, the propagator contains 16 poles, resulting in a 16-fold degeneracy of the spectrum. Following Wilson’s proposal<sup>3</sup>, the degeneracy can be lifted by adding a counterterm (i.e. the Wilson term) to the action which has the effect of pushing the masses of the unwanted doublers to the cut-off scale. However, the Wilson term breaks chiral symmetry explicitly, which has wide-ranging consequences as we shall see below.

Another method for the removal of doubler states is the use of “staggered” or Kogut-Susskind fermions<sup>30</sup>. In this approach, the individual spin components of a Dirac spinor are spread over several lattice sites within a hypercube. Thereby the number of degenerate states is reduced from 16 to 4, which are then interpreted as different flavours. It should be emphasised, however, that the spin/flavour assignment is only valid in the continuum limit. This is different for Wilson fermions, where spin/flavour assignments on the lattice are exactly as in the continuum. This makes the identification of local operators much easier, and therefore the Wilson

formulation appears to be better suited for the study of weak matrix elements of local composite fields. However, staggered fermions leave a  $U(1) \times U(1)$  subgroup of chiral symmetry invariant, and therefore the use of staggered fermions may, after all, be advantageous for studying quantities such as the  $B$  parameter  $B_K$ , whose chiral behaviour is a central issue. As most results for heavy quark physics have been obtained using Wilson quarks, we shall concentrate on this approach in the remainder of this review.

The Wilson action for lattice QCD reads

$$S[U, \bar{\psi}, \psi] = S_G[U] + S_F^W[U, \bar{\psi}, \psi], \quad (9)$$

where

$$\begin{aligned} S_F^W[U, \bar{\psi}, \psi] &= a^4 \sum_x \left\{ -\kappa \sum_{\mu=1}^4 \frac{1}{a} \left[ \bar{\psi}(x)(r - \gamma_\mu)U_\mu(x)\psi(x + \hat{\mu}) \right. \right. \\ &\quad \left. \left. + \bar{\psi}(x + \hat{\mu})(r + \gamma_\mu)U_\mu^\dagger(x)\psi(x) \right] + \bar{\psi}(x)\psi(x) \right\}, \end{aligned} \quad (10)$$

$$\equiv a^4 \sum_{x,y} \bar{\psi}(x) \mathcal{M}(x, y) \psi(y), \quad (11)$$

and in the last line we have introduced the Wilson-Dirac operator  $\mathcal{M}$ . The Wilson term is the piece proportional to  $r$  in the above expression. The hopping parameter  $\kappa$  is related to the bare mass  $m_0$  via

$$\kappa = \frac{1}{2am_0 + 8r}, \quad (12)$$

and the Wilson parameter  $r$  is usually set to one. The Wilson action is thus conveniently parametrised in terms of bare parameters  $(\beta, \kappa)$  instead of the bare gauge coupling and quark mass  $(g_0, m_0)$ . The parametrisation of the fermionic part of the action in eq. (10) implies that the quark and antiquark fields have undergone a rescaling according to

$$\psi(x) \rightarrow \sqrt{2\kappa} \psi(x), \quad \bar{\psi}(x) \rightarrow \bar{\psi}(x) \sqrt{2\kappa}. \quad (13)$$

This normalisation is referred to as the relativistic norm of quark fields.

The addition of the Wilson term proportional to  $r$  to the naïve lattice action leads to an additive renormalisation of the quark mass. This implies that there exists a critical value of the hopping parameter,  $\kappa_{\text{crit}}$ , at which the quark mass vanishes and chiral symmetry is restored. The subtracted quark mass is defined by

$$am = \frac{1}{2} \left( \frac{1}{\kappa} - \frac{1}{\kappa_{\text{crit}}} \right), \quad (14)$$

and in the free theory the critical value of  $\kappa$  occurs at

$$\kappa_{\text{crit}} = \frac{1}{8}, \quad g_0 = 0. \quad (15)$$

The rôle of  $a^{-1}$  as an UV cut-off can also be seen from the fact that at small coupling

$$g_0^2 \sim 1/\ln a, \quad \beta = 6/g_0^2, \quad (16)$$

and therefore the continuum limit,  $a \rightarrow 0$ , is formally reached as  $\beta \rightarrow \infty$ . Note that typical values of the lattice spacing in physical units are  $a^{-1} \simeq 1.5\text{--}4.0$  GeV in current simulations, which corresponds to  $\beta \simeq 5.7\text{--}6.4$ .

By means of the lattice discretisation procedure, one has suitably altered the UV (short-distance) behaviour in order to obtain a non-perturbatively regularised theory, whilst preserving the long-distance physics. The continuum result for, say, hadron masses computed on the lattice is then obtained in the limit  $a \rightarrow 0$ . At this point it is worth noting that the Wilson fermion action differs from the classical continuum action by terms of order  $a$ . In contrast to this, the leading discretisation errors (lattice artefacts) for the pure gauge action are only  $O(a^2)$ , and there are arguments that this is also true for staggered fermions<sup>31</sup>. The predictive power of lattice QCD depends crucially on the degree to which lattice artefacts can be controlled. This is of particular importance for heavy quarks, where the effects due to finite lattice spacing are large, as we shall see below.

The lattice action  $S[U, \bar{\psi}, \psi]$  in eq. (9) can now be used to define a partition function

$$Z = \int D[U] D[\bar{\psi}] D[\psi] e^{-S[U, \bar{\psi}, \psi]}, \quad (17)$$

where, on a finite lattice

$$\int D[U] = \prod_{x, \mu} \int dU_\mu(x), \quad (18)$$

and  $dU_\mu(x)$  is the invariant group measure. The vacuum expectation value (VEV) of an observable  $\mathcal{O}$  is defined as

$$\begin{aligned} \langle \mathcal{O} \rangle &\equiv \frac{1}{Z} \int D[U] D[\bar{\psi}] D[\psi] \mathcal{O} e^{-S_G[U] - S_F^W[U, \bar{\psi}, \psi]} \\ &= \frac{1}{Z} \int D[U] \mathcal{O} \det \mathcal{M}[U] e^{-S_G[U]}, \end{aligned} \quad (19)$$

where in the last equation we have introduced the determinant of the Wilson-Dirac operator by integrating out the fermion fields. The aim of any Monte Carlo simulation is to evaluate  $\langle \mathcal{O} \rangle$  stochastically through an average  $\overline{\mathcal{O}}$  of individual measurements  $\mathcal{O}\{U_i\}$ , computed on a set of gauge configurations  $\{U_i\}$ ,  $i = 1, \dots, N_c$

$$\langle \mathcal{O} \rangle \simeq \overline{\mathcal{O}} = \frac{1}{N_c} \sum_i^{N_c} \mathcal{O}\{U_i\}, \quad (20)$$

where a sequence of  $N_c$  gauge configuration has been generated in a Markov process using  $\det \mathcal{M}[U] e^{-S_G[U]}$  as probability measure. This implies that Monte Carlo results have a statistical error that decreases proportionally to  $1/\sqrt{N_c}$ . In the limit of infinite statistics, the relation between  $\langle \mathcal{O} \rangle$  and  $\overline{\mathcal{O}}$  becomes exact.



If the determinant  $\det \mathcal{M}[U]$  is to be included in the probability measure, then, roughly speaking, it needs to be evaluated in every update step in the Markov chain. Since  $\det \mathcal{M}[U]$  is highly non-local this is prohibitively costly on present computers. Various algorithms have therefore been constructed which should allow for a more efficient evaluation<sup>32,33,34</sup>, but still the computational effort is very large.

It has therefore been proposed to set  $\det \mathcal{M}[U] \equiv 1$  in the generation of gauge configurations, which corresponds to neglecting effects due to quark loops. This procedure defines the so-called *quenched approximation*<sup>35,36</sup>, which is still most widely used in current simulations. Consequently, the overwhelming part of the material covered in this review was obtained using the quenched approximation. As far as hadronic quantities are concerned, the quenched approximation amounts to computing observables in QCD in the presence of a Yang-Mills background field.

We end this subsection with a few more technical remarks. Hadronic observables are extracted from mesonic or baryonic two- or three-point functions, which are constructed from quark propagators  $S_q(x, y)$ . The quark propagators themselves are obtained as the inverse of the Wilson-Dirac operator  $\mathcal{M}$  by solving

$$\mathcal{M}(x, y) S_q(y, z) = \delta_{xz}. \quad (21)$$

Hence, on every gauge configuration  $\{U_i\}$ ,  $i = 1, \dots, N_c$ , one needs to invert the matrix that couples the quark fields in the lattice action. Therefore, the use of an efficient inversion algorithm is of great importance. The most widely used inversion algorithms<sup>37</sup> include the Conjugate Gradient, Minimal Residual and, more recently, the Stabilised Biconjugate Gradient method<sup>38</sup>.

As an example of a mesonic two-point function constructed from quark propagators, we now discuss the euclidean correlation function of the axial current  $A_\mu = \bar{\psi} \gamma_\mu \gamma_5 \psi$ , which is used to extract properties of pseudoscalar mesons. For euclidean times  $t \equiv x_4 > 0$ , the correlation function is defined by

$$C(t; \vec{p}) \equiv \sum_{\vec{x}} e^{-i\vec{p} \cdot \vec{x}} \langle 0 | A_4(\vec{x}, t) A_4^\dagger(0) | 0 \rangle, \quad (22)$$

which, after performing the Wick contractions, can be written in terms of quark propagators  $S_q(y, x)$  as

$$C(t; \vec{p}) \equiv - \sum_{\vec{x}} e^{-i\vec{p} \cdot \vec{x}} \langle \text{Tr} \{ \gamma_4 S_q(0, x) \gamma_4 S_q^\dagger(0, x) \} \rangle. \quad (23)$$

Here we have used that  $S_q(x, 0) = \gamma_5 S_q^\dagger(0, x) \gamma_5$ . Inserting a complete set of intermediate states in eq. (22), one obtains the spectral decomposition of the correlation function, viz.

$$C(t; \vec{p}) = \sum_n \frac{|\langle 0 | A_4(0) | n; \vec{p} \rangle|^2}{2E_n(\vec{p})} e^{-E_n(\vec{p})t}. \quad (24)$$

For large  $t$ , the lightest state in the spectral decomposition dominates. For  $\vec{p} = 0$ , the asymptotic form of  $C(t; \vec{p})$  is given by

$$C(t; \vec{0}) \stackrel{t \gg 0}{\approx} \frac{|\langle 0 | A_4(0) | P \rangle|^2}{2M_P} e^{-M_P t}, \quad (25)$$

where  $M_P$  is the mass of the pseudoscalar meson in the ground state.

In order to obtain reliable estimates of the mass  $M_P$  and the matrix element  $\langle 0|A_4(0)|P\rangle$  in a lattice calculation, one has to be able to follow the signal for  $C(t; \vec{0})$  up to large  $t$ , which requires good statistics. Furthermore, the lattice has to be long enough for the lightest state to be observable, and therefore one normally chooses  $T = 2L$ . For heavy quark systems, the issue of reaching the asymptotic behaviour of  $C(t; \vec{0})$  is a particular problem; here, the correlation function falls off rapidly and may have dived into the statistical noise before the ground state can be observed. Therefore, one has to choose operators in the evaluation of  $C(t; \vec{0})$  which have a good overlap onto the ground state. Using point-like, local operators such as  $\bar{\psi}(x)\gamma_\mu\gamma_5\psi(x)$  above, results in a very poor signal. This can be intuitively understood from the fact that the wave function of the particle one wants to study is an extended object and not point-like. Therefore, when solving for the quark propagators, eq. (21), one applies so-called *smearing techniques*, which are designed to generate more extended sources, having a better overlap onto the desired state<sup>40–42,44,98,118,128</sup>. Since the signal-to-noise ratio for hadron masses and decay constants can be enormously improved using “smeared” sources and/or sinks in the propagator calculation, smearing techniques are now an indispensable tool in lattice simulations of QCD.

In a simulation, dimensionful quantities like hadron masses or pseudoscalar decay constants are obtained in lattice units. In order to convert these lattice estimates into physical units, one needs to set the lattice scale. This is usually done by comparing a low-energy hadronic quantity computed on the lattice to its physical value. For instance, using the mass of the  $\rho$  meson one obtains  $a^{-1}$  [GeV] via

$$a^{-1} [\text{GeV}] = \frac{M_\rho [\text{GeV}]}{(aM_\rho)}, \quad (26)$$

where  $aM_\rho$  denotes the lattice result for the  $\rho$  mass. Other quantities used to set the scale include the pion decay constant  $f_\pi$ , the nucleon mass, the string tension  $\sqrt{\sigma}$  or the hadronic scale  $r_0$  discussed by Sommer<sup>45</sup>.

One complication that arises in the computation of  $aM_\rho$  (and, indeed, of all quantities that involve  $u$  and  $d$  quarks), is that one cannot simulate directly at the  $u$  and  $d$  quark masses. This comes from the fact that hadronic quantities involving very light quarks have large correlation lengths, which would lead to severe finite-size effects on currently accessible lattice sizes. Therefore, one typically uses quark masses in the region of that of the strange quark and extrapolates the results to  $m_{u,d}$ , or to the chiral limit. Finite-size effects are discussed in more detail in subsection 2.4.

## 2.2. The $b$ quark on the lattice

As already mentioned in subsection 2.1, current simulations are carried out at typical values of the inverse lattice spacing in physical units of  $a^{-1} \simeq 1.5\text{--}4$  GeV. For heavy quarks, this implies that one needs to worry about the effects of finite cut-off already when one wants to study charm physics, since  $m_{\text{charm}}$  is only about a

factor of two smaller than  $a^{-1}$ . Furthermore, it is evident that the  $b$  quark cannot be studied directly, since its Compton wavelength is smaller than the lattice spacing. Hence, one concludes that lattice artefacts are large for heavy quarks, and that special care is required to control them.

In the following we describe several methods which are employed to circumvent the problem that the  $b$  quark cannot be studied directly or are designed to alleviate the problem of large discretisation errors.

### 2.2.1. $O(a)$ improvement

In this approach one seeks to reduce lattice artefacts by using so-called *improved* actions and operators in order to cancel the leading discretisation error in on-shell quantities. The concept of perturbative improvement was first outlined by Symanzik<sup>46</sup> and developed further in refs.<sup>47–49</sup>. For the Wilson action in lattice QCD, Sheikholeslami and Wohlert have shown that the  $O(a)$  discretisation error in the action can be cancelled by adding a local counterterm<sup>48</sup>

$$S_{SW}[U, \bar{\psi}, \psi] = S_G[U] + S_F^W[U, \bar{\psi}, \psi] + c_{sw} \frac{i}{4} a^5 \sum_{x, \mu, \nu} \bar{\psi}(x) \sigma_{\mu\nu} F_{\mu\nu}(x) \psi(x), \quad (27)$$

where the improvement coefficient  $c_{sw}$  depends on the gauge coupling. In order to obtain  $O(a)$  improved matrix elements of composite operators, these composite fields have to be improved, too<sup>49,50</sup>. For instance, the improved axial current reads

$$A_\mu^I(x) = A_\mu(x) + c_A a \partial_\mu P(x), \quad (28)$$

where  $A_\mu(x) = \bar{\psi}(x) \gamma_\mu \gamma_5 \psi(x)$ ,  $P(x) = \bar{\psi}(x) \gamma_5 \psi(x)$ , and  $c_A$  denotes another improvement coefficient. Recently, the ALPHA Collaboration<sup>50,51,52</sup> has proposed an  $O(a)$  improved action for which the improvement coefficients  $c_{sw}$  and  $c_A$  were determined non-perturbatively for  $\beta \geq 6.0$ . This action has so far not been used in simulations of heavy quark systems.

### 2.2.2. Non-relativistic normalisation

In a second approach, it has been suggested<sup>55–58</sup> to suitably adapt the Wilson action, such that the Wilson propagator does not deviate from the continuum behaviour even for quark masses  $am \gtrsim 1$  in lattice units (i.e. for quark masses above the cut-off). It has been argued that this can be achieved by a modified rescaling of lattice quark fields (c.f. eq. (13)) according to

$$\psi(x) \rightarrow \sqrt{2\kappa} e^{am_P/2} \psi(x), \quad (29)$$

where the “pole mass”  $am_P$  of the Wilson propagator is given by

$$am_P = \ln(1 + am), \quad (30)$$

and  $am$  is defined in eq. (14). The factor  $\sqrt{2\kappa} e^{am_P/2}$  is designed to interpolate smoothly between the relativistic and non-relativistic regimes.

Consequently, in order to cancel the effects of large quark masses in studies of matrix elements of composite operators, the normalisation of quark fields is changed according to the above scale factor. This non-relativistic normalisation of quark fields according to eq. (29) is referred to as the Kronfeld-Lepage-Mackenzie (KLM) norm.

Higher-order corrections for large quark masses can also be considered. As is argued in <sup>54,55,56</sup>, this can be motivated by the observation that for quark masses  $am > 1$ , the mass  $am_P$  and the “kinetic mass”  $am_2$  appearing in the non-relativistic dispersion relation, are no longer equal

$$aE(\vec{p}) = am_P + \frac{\vec{p}^2}{2am_2} + \dots, \quad m_2 \neq m_P, \quad (31)$$

and the relevant quark mass is the kinetic mass  $m_2$ . In the free theory, the kinetic mass  $am_2$  is obtained from the free Wilson propagator in the non-relativistic limit

$$am_2 = \frac{e^{am_P} \sinh(am_P)}{\sinh(am_P) + 1}. \quad (32)$$

Both  $O(a)$  improvement and the KLM norm are used for quark masses in the region of that of the charm quark. Clearly, residual lattice artefacts remain and must ultimately be extrapolated away (which, however, can be performed much more reliably if they are small). The results obtained around  $m_{\text{charm}}$  must also be extrapolated to the mass of the  $b$  quark, and clearly one needs to control this extrapolation in order to obtain meaningful results. In what follows, we shall refer to this approach, where relativistic heavy quarks are used in conjunction with a prescription to reduce lattice artefacts (either  $O(a)$  improvement or the KLM-norm), as the “conventional method”.

### 2.2.3. Static approximation

Here the  $b$  quark is treated as infinitely heavy <sup>7</sup>. From an expansion of the heavy quark propagator in the inverse heavy quark mass,  $1/m_Q$ , one obtains at leading order <sup>9</sup>

$$S_Q(\vec{x}, t; \vec{0}, 0) = \left\{ \Theta(t) e^{-m_Q t} \frac{1 + \gamma_4}{2} + \Theta(-t) e^{m_Q t} \frac{1 - \gamma_4}{2} \right\} \delta(\vec{x}) \mathcal{P}_{\vec{0}}(t, 0), \quad (33)$$

where  $\mathcal{P}_{\vec{0}}(t, 0)$  is the product of links from  $(\vec{0}, t)$  to the origin, for example for  $t > 0$ ,

$$\mathcal{P}_{\vec{0}}(t, 0) = U_4^\dagger(\vec{0}, t-1) U_4^\dagger(\vec{0}, t-2) \cdots U_4^\dagger(\vec{0}, 0). \quad (34)$$

This form of the propagator is also obtained using a Lagrangian for heavy quarks  $Q(x)$  which simply reads <sup>60</sup>

$$\mathcal{L}^{\text{static}} = Q^\dagger(x) D_4 Q(x), \quad (35)$$

where the covariant derivative is defined in eq. (6), and  $Q(x)$  is a two-component spinor describing the heavy quark.

One expects corrections of order  $\Lambda_{\text{QCD}}/m_Q$  to the results in the static approximation, which can potentially be large. With a few exceptions, such as the  $B^*-B$  mass splitting, the computation of higher order corrections in  $1/m_Q$  to the static limit is complicated due to the presence of power divergencies<sup>69</sup>. Nevertheless, the static approximation is a valuable tool in lattice studies of heavy quark systems. It plays the crucial rôle of guiding the extrapolation of results obtained with the conventional method to the mass of the  $b$  quark by providing direct information at infinite quark mass.

#### 2.2.4. Non-relativistic QCD (NRQCD)

A non-relativistic formulation of heavy quark systems<sup>70</sup> can be obtained by excluding relativistic momenta through the introduction of a finite cut-off  $\Lambda_{\text{UV}} \lesssim m_Q$  such that

$$p \sim m_Q v \ll m_Q, \quad (36)$$

where  $v$  is the 4-velocity of the heavy quark. The loss of relativistic states through this requirement can be compensated for by adding new local interactions order by order in  $p/\Lambda_{\text{UV}}$ . In this way one obtains a cut-off theory as an expansion of the original action in  $p/\Lambda_{\text{UV}} \sim v$ . The non-relativistic QCD Lagrangian is then obtained by applying a Foldy-Wouthuysen transformation, which separates quark and antiquark fields, thereby generating an expansion of the QCD Lagrangian in  $1/m_Q$ . For instance, at order  $1/m_Q$  the NRQCD Lagrangian reads

$$\mathcal{L}^{\text{NRQCD}} = Q^\dagger \left( D_4 - \frac{\vec{D}^2}{2m_Q} \right) Q - Q^\dagger \frac{\vec{\sigma} \cdot \vec{B}}{2m_Q} Q. \quad (37)$$

This approach is thus based on the *a priori* discretisation of the non-relativistic formulation of the Wilson action. Although the above expression contains the term that defines  $\mathcal{L}^{\text{static}}$  in eq. (35), one should realise that there are important differences between NRQCD and the static approximation: the theory defined by the NRQCD Lagrangian is non-renormalisable, since a finite cut-off has to be kept

$$\Lambda_{\text{UV}} \sim a^{-1} \lesssim m_Q. \quad (38)$$

In the language of the lattice this means that the formal continuum limit,  $a \rightarrow 0$ , does not exist, in contrast to the case of the static approximation. Hence, for NRQCD to work in a lattice simulation, one needs to calculate at fairly large values of  $a$  (i.e. at small  $\beta$ ). Lattice artefacts (i.e. cut-off effects) have to be reduced by including higher orders in  $1/m_Q$ . For the study of matrix elements of composite fields using NRQCD to  $n$ th order in  $1/m_Q$ , it is important to take into account corrections of  $O(1/m_Q^n)$  in the operators as well.

From the above discussion of various methods to formulate heavy quarks on the lattice, it is obvious that none of them is entirely satisfactory. They are subject to rather different systematic effects and thus provide complementary information on

heavy quark systems. The full picture will therefore only emerge when results from all methods are compared.

### 2.3. *Weak matrix elements on the lattice and their continuum counterparts*

It has already been noted in subsection 2.1 that the Wilson action in eq. (10) breaks chiral symmetry explicitly. Therefore, even in the massless theory, vector and axial vector currents are not conserved, since the UV behaviour of the theory has been changed as a consequence of the regularisation procedure. In other words, the regularisation procedure conflicts with the naïve conservation of the currents. The resulting short-distance corrections between the vector and axial currents in lattice and continuum theories can be absorbed into normalisation factors  $Z_V$  and  $Z_A$ , respectively.

The chiral Ward identities for the axial current normally ensure that the axial current does not get renormalised. However, since chiral symmetry is broken explicitly by the Wilson term, the Ward identity no longer applies, as it is violated by terms of order  $a$ . Nevertheless, the condition that the correctly normalised lattice axial current satisfies the Ward identities can be used to derive its normalisation<sup>71,72</sup>. Since the normalisation factors incorporate short-distance effects, they can in principle be calculated in lattice perturbation theory.

Using the unimproved Wilson action the one-loop perturbative results for the vector and axial current normalisation constants read<sup>73,74,75</sup>

$$Z_A = 1 - 0.133 g_0^2 + O(g_0^4), \quad Z_V = 1 - 0.174 g_0^2 + O(g_0^4), \quad (39)$$

whereas for the  $O(a)$  improved Sheikholeslami-Wohlert action\*, eq. (27) one obtains<sup>76,77</sup>

$$Z_A = 1 - 0.018 g_0^2 + O(g_0^4), \quad Z_V = 1 - 0.100 g_0^2 + O(g_0^4). \quad (40)$$

These expressions are written in terms of the bare gauge coupling  $g_0^2$ , which is given by  $g_0^2 = 6/\beta$ . However, it has been argued in<sup>57</sup> that the bare gauge coupling is a bad expansion parameter due to the appearance of large gluonic tadpole contributions in the relation between the link variable  $U_\mu(x)$  and the continuum gauge field  $A_\mu(x)$  (see eq. (4)). The poor convergence property of lattice perturbation theory can be improved by absorbing these tadpole contributions into suitable redefinitions of the bare parameters of the theory. The simplest definition of an improved expansion parameter is the so-called “boosted” coupling  $\tilde{g}^2$  introduced by Parisi<sup>78</sup>

$$\tilde{g}^2 \equiv \frac{g_0^2}{u_0^4}, \quad (41)$$

where  $u_0^4$  is taken to be the measured average value of the plaquette  $\langle \frac{1}{3} \text{Re Tr } P \rangle$  ( $u_0 = \langle \frac{1}{3} \text{Re Tr } P \rangle^{1/4}$  is a gauge invariant estimate of the average link). Replacing

\*Note that here we quote the expressions for the non-local currents which have been “rotated” according to the prescription given in<sup>49,77</sup>.

the bare coupling  $g_0^2$  by  $\tilde{g}^2$  in the one-loop expressions for  $Z_A$  and  $Z_V$  defines the so-called “boosted” perturbation theory.

In the fermionic sector, one can absorb tadpole contributions into a redefinition of the hopping parameter  $\kappa$  in a similar fashion according to

$$\tilde{\kappa} \equiv \kappa u_0. \quad (42)$$

It is then expected that the critical value of  $\tilde{\kappa}$  is much closer to its tree-level value of  $1/8$ , such that  $u_0 \simeq 1/8\kappa_{\text{crit}}$ , c.f. eq. (15). This is the basic concept of *tadpole* or *mean field* improvement<sup>57</sup>. By using non-perturbative input for  $u_0$  such as the measured link or, alternatively,  $\kappa_{\text{crit}}$ , one can improve the UV behaviour of the lattice theory, which should manifest itself in a better convergence of lattice perturbation theory.

Tadpole improved expressions for the normalisation factors are obtained by combining their perturbation expansions with those for  $u_0$  as well as the measured value of the latter<sup>57</sup>. For instance, the tadpole improved one-loop expression for the axial current normalisation reads

$$\tilde{Z}_A = u_0 \left( 1 + [Z_A^{(1)} - u_0^{(1)}] \tilde{g}^2 \right), \quad (43)$$

where  $Z_A^{(1)}$  and  $u_0^{(1)}$  are the one-loop coefficients in the expansions of  $Z_A$  and  $u_0$ , respectively. The numerical value of  $u_0^{(1)}$  depends on whether one identifies  $u_0$  with the average link or the critical hopping parameter, thus considering the perturbative expansions of either  $\langle \frac{1}{3} \text{Re Tr } P \rangle^{1/4}$  or  $8\kappa_{\text{crit}}$ .

In conjunction with the KLM-norm defined in eq. (29), tadpole improvement also plays an important rôle in reducing lattice artefacts due to large quark masses. As an example we consider the case of the lattice axial current  $\bar{\psi}_1 \gamma_\mu \gamma_5 \psi_2$  of quark fields  $\psi_1, \psi_2$  with hopping parameters  $\kappa_1$  and  $\kappa_2$ , respectively. The normalisation factor of the axial current is then supplemented by an extra factor of

$$\exp\{a(m_{\text{P},1} + m_{\text{P},2})/2\}, \quad (44)$$

which arises from the modified rescaling of quark fields in eq. (29). Inserting the definition of the pole mass and applying tadpole improvement, the normalisation factor becomes

$$\begin{aligned} e^{a(\tilde{m}_{\text{P},1} + \tilde{m}_{\text{P},2})/2} \tilde{Z}_A &= \sqrt{\left(1 + \frac{1}{2\tilde{\kappa}_1} - \frac{1}{2\tilde{\kappa}_{\text{crit}}}\right) \left(1 + \frac{1}{2\tilde{\kappa}_2} - \frac{1}{2\tilde{\kappa}_{\text{crit}}}\right)} \tilde{Z}_A \\ &= \sqrt{\left(\frac{1}{2\tilde{\kappa}_1} - 3\right) \left(\frac{1}{2\tilde{\kappa}_2} - 3\right)} \tilde{Z}_A, \end{aligned} \quad (45)$$

where in the last step we have used  $\tilde{\kappa}_{\text{crit}} = \kappa_{\text{crit}} u_0 \simeq 1/8$ , a relation that becomes exact if  $u_0$  is defined by  $1/8\kappa_{\text{crit}}$  rather than the average link.

Apart from the coupling constant defined in eq. (41) other definitions of a mean field improved coupling can be used. Lepage and Mackenzie<sup>57</sup> proposed a coupling

$\alpha_V$  defined through

$$\alpha_V(3.41a^{-1})\left(1 - (1.19 + 0.017n_f)\alpha_V\right) = -\frac{3}{4\pi} \ln\left\langle \frac{1}{3} \text{Re Tr} P \right\rangle. \quad (46)$$

If  $\alpha_V$  is to be used for the evaluation of a tadpole improved normalisation factor, then, according to ref. <sup>57</sup>, it has to be computed at a scale  $q^*$ , which denotes the mean momentum flow relevant for a given matrix element. Typical values of  $q^*$  lie in the range  $1 \leq aq^* \leq \pi$ .

Given the potential uncertainty in the perturbative expressions from higher orders, it is desirable to perform non-perturbative determinations of the normalisation factors. For  $Z_A$  and  $Z_V$  this can be done by imposing the chiral Ward identities as a normalisation condition <sup>72,79,80,81</sup>. A more general approach, which can be applied to a large class of operators <sup>82</sup>, imposes the normalisation condition between quark states. Numerical values have so far been obtained for the axial current for  $c_{\text{sw}} = 0$  <sup>83</sup>, in the static approximation for  $c_{\text{sw}} = 1$  <sup>84</sup>, and also for the  $\Delta S = 2$  four-fermion operator relevant for the Kaon  $B$  parameter  $B_K$  <sup>84,85</sup>. Systematic errors in non-perturbative determinations of normalisation factors are, of course, present and need to be controlled. Recently, the ALPHA Collaboration <sup>53</sup> has determined  $Z_A$  and  $Z_V$  non-perturbatively in the whole range  $0 \leq g_0^2 \leq 1$ , with total errors at the 1% level.

Apart from the problem of the normalisation of lattice operators, another consequence of explicit chiral symmetry breaking is the possibility of mixing of operators with a definite chirality. For instance, the  $\Delta F = 2$  four-fermion operator defined by

$$\hat{O}_L \equiv (\bar{\psi}\gamma_\mu(1 - \gamma_5)\psi) (\bar{\psi}\gamma_\mu(1 - \gamma_5)\psi) \quad (47)$$

can mix with its right-handed counterpart

$$\hat{O}_R \equiv (\bar{\psi}\gamma_\mu(1 + \gamma_5)\psi) (\bar{\psi}\gamma_\mu(1 + \gamma_5)\psi). \quad (48)$$

Furthermore, operators can mix with higher dimension operators, which is also a consequence of the breaking of Lorentz invariance by formulating QCD on a hypercubic lattice.

Hence, in general the relation between the matrix element of an operator  $\hat{O}$  in the continuum and in the Wilson formulation is given by

$$\langle f|\hat{O}|i\rangle^{\text{cont}} = \sum_{\alpha} Z_{\alpha} \langle f|\hat{O}_{\alpha}^{\text{latt}}|i\rangle + O(a), \quad (49)$$

where  $\alpha$  labels the operators of the same dimension that can mix with each other, and  $Z_{\alpha}$  are the short-distance normalisation factors.

#### 2.4. *Summary of systematic errors*

The main systematic effects that affect lattice results for heavy quark physics can be broadly divided into lattice artefacts, finite-size effects, quenching errors and normalisation of lattice operators.



In any simulation in physical volumes, the following inequalities must be satisfied

$$a \ll M^{-1} \ll L, \quad (50)$$

where  $M$  is a typical hadronic mass, and  $L$  denotes the spatial length of the lattice. The left part of the inequality constrains the possible values of heavy quark masses that can be studied safely, i.e. without suffering from large discretisation errors. On the other hand, very light quark masses will give rise to finite-size effects, as is evident from the right part of the above inequality. Hence, a major limitation of current lattice simulations is that very different scales need to be incorporated on a single lattice.

We now list and discuss the main systematic errors which affect lattice results for heavy quark systems:

#### 2.4.1. Discretisation errors

Discretisation errors, i.e. the effects of the finiteness of the lattice spacing, are present in all simulations of lattice QCD, but are especially important for heavy quark systems as we have seen in subsection 2.2. We have already discussed how  $O(a)$  improvement can be used to reduce these effects, and there are attempts to extend the improvement programme beyond  $O(a)$ <sup>86,87</sup> or to even construct “perfect” lattice actions that ideally are completely free of discretisation errors<sup>88,89,90</sup>. Once these cut-off effects are reduced, either by employing the Symanzik improvement programme or by absorbing effects of large quark masses into the normalisation of quark fields (KLM-norm), residual discretisation errors have to be extrapolated away by taking the limit  $a \rightarrow 0$ .

It should be emphasised that this procedure does *not* solve the problem that the  $b$  quark cannot be studied directly in current simulations using relativistic quarks.

#### 2.4.2. Finite-size effects

Lattice estimates of hadron masses and matrix elements are distorted due to the finiteness of the lattice volume. An analytic calculation by Lüscher<sup>91</sup> showed that the mass shift in finite volume decreases exponentially with  $L$

$$\delta M(L) \equiv M(L) - M(\infty) \sim e^{-L/L_0}. \quad (51)$$

Numerical studies, however, revealed that for spatial lengths of  $L \lesssim 2.0$  fm the observed mass shift deviates from the exponential decrease and is very well described by a power law behaviour. Using a simple model, the effect can be ascribed to the “squeezing” of hadronic wave functions for small volumes<sup>92,93</sup>, and for values of  $L \gtrsim 2$  fm, one recovers the exponential behaviour of eq. (51).

In practice one obtains estimates of hadronic observables in infinite volume by repeating the simulations at different values of  $L$  and extrapolating to the infinite volume limit.

Finite-size effects also prevent light quark propagators from being calculated at realistic values of the masses of  $u$  and  $d$  quarks, whose bound states have large

correlation lengths. Therefore, light quark masses are usually taken around the mass of the strange quark, and hadronic observables are then extrapolated to the chiral limit, using the quark mass dependence deduced from chiral perturbation theory as a guide for the extrapolation.

#### 2.4.3. *Quenching*

As most lattice results for heavy quark systems are still obtained in the quenched approximation, attempts must be made to quantify the effects due to neglecting quark loops, in order to provide meaningful information for phenomenology. In the past few years, several collaborations have reported results for heavy quark physics using dynamical quarks, but much more precise simulations have yet to be performed.

An indirect manifestation of quenching effects is the uncertainty in the lattice scale  $a^{-1}$  [GeV]. This uncertainty arises because different quantities used to set the scale give different results, which is understood from the fact that quark loops make different contributions to the various quantities used to compute  $a^{-1}$  [GeV].

#### 2.4.4. *Normalisation and mixing of lattice operators*

Uncertainties in the normalisation factors relating lattice matrix elements to their continuum counterparts come from the fact that these factors are, in most cases, only known perturbatively to leading order in  $g_0^2$ . In a few cases, e.g. for the heavy-light axial current in the static approximation, this uncertainty may be of the order of 10%. Non-perturbative estimates of these constants are therefore highly desirable. For vector and axial vector currents the chiral Ward identities can easily be employed as normalisation conditions in a non-perturbative determination. For more complicated operators or scale-dependent renormalisations, a more general condition needs to be applied<sup>82</sup>, which, however, may be less accurate numerically.

In order to check the consistency of different methods, one needs to make contact between perturbative and non-perturbative estimates of normalisation constants. If  $g_0^2$  is used as an expansion parameter in the evaluation of the perturbative expressions, this is only possible at large values of  $\beta$ , where non-perturbative methods normally fail. Using a “boosted” or tadpole-improved coupling  $\tilde{g}^2$  instead, one may try to make a comparison in a region where current simulations are being performed. In some cases it was found that “boosted” perturbation theory yields values close to the non-perturbative determinations, but the issue remains inconclusive as long as small values of the couplings cannot be investigated numerically. A systematic non-perturbative analysis for  $0 \leq g_0^2 \leq 1$  has been performed in the framework of the Schrödinger functional<sup>52,53</sup>.

### 3. **Leptonic Decays of Heavy Mesons**

In this section we review lattice results for heavy-light decay constants such as  $f_D$ ,  $f_{D_s}$ ,  $f_B$  and  $f_{B_s}$ . After introducing the basic definitions, we present and discuss

the results obtained using different formulations of heavy quarks on the lattice. Subsection 3.4 contains a detailed discussion of the approach of the continuum limit for unimproved Wilson fermions. Readers who are not interested in the details of the continuum extrapolation will find the main results listed in subsection 3.5, where also a comparison to other theoretical methods is presented. Throughout this review we use a convention for which  $f_\pi = 131$  MeV.

### 3.1. Basic definitions

In the continuum, the pseudoscalar decay constant  $f_P$  is defined by

$$\langle 0 | A_\mu(0) | P(\vec{p}) \rangle = i p_\mu f_P, \quad (52)$$

whereas the vector decay constant  $1/f_V$  is usually defined by

$$\langle 0 | V_\mu(0) | V \rangle = \epsilon_\mu \frac{M_V^2}{f_V}. \quad (53)$$

Hence, in order to extract the decay constants of heavy-light mesons, one needs to compute the matrix elements of the axial and vector currents between a mesonic state and the vacuum.

On a lattice, this is achieved by analysing various mesonic two-point functions of the form

$$C_{J_1 J_2}^{QR}(t) \equiv \sum_{\vec{x}} \langle 0 | J_1^Q(x) J_2^{\dagger R}(0) | 0 \rangle, \quad (54)$$

where  $J_1$  and  $J_2$  are interpolating operators which can annihilate or create the heavy-light pseudoscalar or vector meson under study. The superscripts  $Q, R$  denote whether a local ( $L$ ) or smeared ( $S$ ) interpolating operator is used.

One possibility to extract the heavy-light pseudoscalar decay constant is to consider the ratio

$$\begin{aligned} \frac{C_{AP}^{LS}(t)}{C_{PP}^{SS}(t)} &\equiv \frac{\sum_{\vec{x}} \langle 0 | A_4^L(\vec{x}, t) P^{\dagger S}(0) | 0 \rangle}{\sum_{\vec{x}} \langle 0 | P^S(\vec{x}, t) P^{\dagger S}(0) | 0 \rangle} \\ &\stackrel{t \gg 0}{\sim} \frac{\langle 0 | A_4^L(0) | P \rangle}{\langle 0 | P^S(0) | P \rangle} \tanh(M_P(T/2 - t)), \end{aligned} \quad (55)$$

where we have used the expressions for the asymptotic behaviour for both  $C_{AP}^{LS}(t)$  and  $C_{PP}^{SS}(t)$  on a finite lattice with time extension  $T$  and periodic boundary conditions. Using the smeared pseudoscalar density  $P^S(x)$  to create the pseudoscalar meson in  $C_{AP}$  and  $C_{PP}$  results in a much better signal for these correlation functions. This is of particular importance in the static approximation discussed below, where it is notoriously difficult to obtain a reliable signal, and where calculations using purely local operators are known to fail<sup>42,43,94,134</sup>.

In order to determine  $\langle 0 | A_4^L(0) | P \rangle$  which contains the decay constant, one also needs to know the pseudoscalar mass  $M_P$  and the matrix element  $\langle 0 | P^S(0) | P \rangle$ ,

which are extracted from separate fits to

$$C_{PP}^{SS}(t) \stackrel{t \gg 0}{\sim} \frac{|\langle 0|P^S(0)|P \rangle|^2}{2M_P} e^{-M_P T/2} \cosh(M_P(T/2 - t)). \quad (56)$$

From  $\langle 0|A_4^L(0)|P \rangle$  one can then extract  $f_P$  via

$$\langle 0|A_4^L(0)|P \rangle = M_P f_P / Z_A, \quad (57)$$

where  $Z_A$  is the normalisation constant of the axial current discussed in subsection 2.3, which is usually evaluated in (“boosted” or tadpole-improved) perturbation theory. The actual value of  $Z_A$  depends on whether an improved action has been used (i.e. on the choice of  $c_{\text{sw}}$ ), on the details of the implementation of tadpole improvement, and also on whether the relativistic, non-relativistic or static formulation of heavy quarks has been used.

In the two-spinor formalism of the static approximation (see eq. (35)), there is no distinction between  $A_4(x)$  and  $P(x)$ , such that the pseudoscalar decay constant is extracted from combinations of the following correlation functions

$$C^{SS}(t) = \sum_{\vec{x}} \langle 0|A_4^S(\vec{x}, t) A_4^{\dagger S}(0)|0 \rangle \stackrel{t \gg 0}{\sim} (A^S)^2 e^{-\mathcal{E}t}, \quad (58)$$

$$C^{SL}(t) = \sum_{\vec{x}} \langle 0|A_4^S(\vec{x}, t) A_4^{\dagger L}(0)|0 \rangle \stackrel{t \gg 0}{\sim} A^S A^L e^{-\mathcal{E}t}, \quad (59)$$

where  $\mathcal{E}$  is the unphysical difference between the meson mass and the mass of the heavy quark. The decay constant  $f_B^{\text{stat}}$  is related to the matrix element  $A^L$  via

$$f_B^{\text{stat}} = A^L \sqrt{2/M_B} Z_A^{\text{stat}}. \quad (60)$$

The one-loop expressions for  $Z_A^{\text{stat}}$  were calculated in refs. <sup>59,60,61</sup>, and later extended to the  $O(a)$  improved case <sup>62,63</sup>. Here we do not list the expressions but refer the reader to appendix A, where we have listed the normalisation factors for some operators of interest.

A similar procedure as the one described above can be applied to determine the vector decay constant  $1/f_V$ .

### 3.2. Decay constants and heavy quark symmetry

Lattice results for decay constants using the conventional or non-relativistic formulations can be used to test predictions of the Heavy Quark Effective Theory. It is well known that HQET predicts a scaling law for heavy-light decay constants in the limit of infinite quark mass,  $m_Q \rightarrow \infty$

$$\frac{M}{f_V} \sim f_P \sim \frac{\text{const}}{\sqrt{M}} \alpha_s^{-2/\beta_0}, \quad (61)$$

where  $M_P \sim M_V \sim M \sim m_Q$ . Hence, the heavy quark flavour symmetry implies that  $f_P \sqrt{M_P}$  behaves like a constant (up to logarithmic corrections)

$$f_P \sqrt{M_P} \sim \text{const} \alpha_s^{-2/\beta_0}, \quad (62)$$

where  $\beta_0 = 11 - \frac{2}{3}n_f$ , and  $n_f$  is the number of active quark flavours. The heavy quark spin symmetry predicts the vector and pseudoscalar decay constants to be degenerate. Defining  $U(M)$  as the ratio of matrix elements of the axial and vector currents one expects

$$U(M) \equiv \frac{f_V f_P}{M} \sim 1, \quad m_Q \rightarrow \infty. \quad (63)$$

In order to study the mass dependence of  $f_P \sqrt{M_P}$ , one divides out the scaling factor  $\alpha_s^{-2/\beta_0}$  and defines the quantity

$$\Phi(M_P) \equiv f_P \sqrt{M_P} \left( \frac{\alpha_s(M_P)}{\alpha_s(M_B)} \right)^{2/\beta_0}. \quad (64)$$

In figure 1 we compare some results for  $\Phi(M_P)$  obtained using the static approximation<sup>98,99,100</sup> with those from the conventional formulation<sup>99,101,102</sup>. One observes rather high values in the static approximation, whereas the results using relativistic heavy quarks are much lower. The figure also illustrates that improvement is a crucial ingredient for detecting deviations from the scaling law: using either the Sheikholeslami-Wohlert (SW) action in eq. (27) or employing the KLM-norm, it seems possible to interpolate between the static approximation and the conventional approach. Using the standard relativistic norm in eq. (13) instead leads first to a flattening and then to a decrease of  $\Phi(M_P)$  as the heavy quark mass is increased, as is shown in figure 1 using the results of the PSI-CERN-Wuppertal (PCW) group<sup>102</sup>. Hence, the infinite mass limit of  $\Phi(M_P)$  would be in complete disagreement with the results obtained directly at infinite  $b$  quark mass. Figure 1 also illustrates our earlier remark that different formulations of heavy quarks have to be used simultaneously in order to reveal the full picture. Another remarkable observation is that results from simulations with different systematics agree very well within errors (at similar values of the lattice spacing), which underlines the consistency of the different methods.

From the slope of  $\Phi(M_P)$  one can infer the size of  $1/M_P$  corrections to the scaling law, eq.(62). They amount to about 15% at the mass of the  $B$  meson and about 40% at the mass of the  $D$ . Thus it appears that there are large corrections to the predictions of the heavy quark flavour symmetry for decay constants. Recent studies using NRQCD<sup>104–108</sup> have reported even larger corrections at  $M_B$ .

A test of the heavy quark spin symmetry can be performed by computing the quantity  $U(M)$  and studying its mass dependence. In the heavy quark limit,  $U(M)$  differs from one by short-distance corrections<sup>95–97</sup>

$$U(M) \equiv \frac{f_V f_P}{M} = \left( 1 + \frac{8}{3} \frac{\alpha_s(M)}{4\pi} + O(1/M) \right). \quad (65)$$

The UKQCD collaboration performed this analysis using the  $O(a)$  improved SW action; the short-distance corrections were divided out, and the resulting data were fitted to either a linear or quadratic function of the inverse, spin-averaged mass  $1/M$ .

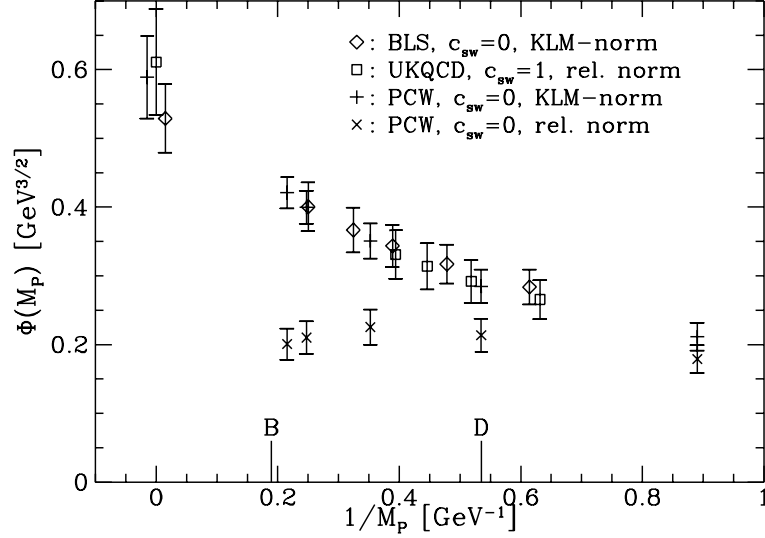


Fig. 1. The quantity  $\Phi(M_P)$  plotted against the inverse pseudoscalar mass. Diamonds represent the data from ref. <sup>99</sup>, obtained at  $\beta = 6.3$ , squares denote the results from UKQCD <sup>101,100</sup>, using the SW action at  $\beta = 6.2$ . The data from refs. <sup>98,102</sup> at  $\beta = 6.26$  are represented by plus signs (KLM-norm) and crosses (relativistic norm). The data obtained in the static approximation are slightly shifted for clarity. Also the positions of the  $B$  and  $D$  meson masses are indicated.

Figure 2 shows that  $U(M)$  indeed is consistent with one in the heavy-quark limit. This result demonstrates not only the manifestation of the heavy-quark spin symmetry in the infinite mass limit, it also provides support for the parametrisation of the non-scaling behaviour of  $f_P\sqrt{M_P}$  as a power series in  $1/M_P$ .

Despite these encouraging results, heavy quark scaling laws for decay constant require further investigation. In particular, the size of  $1/M$  corrections has to be studied as one approaches the continuum limit, in order to detect to what extent the slope in  $f_P\sqrt{M_P}$  is influenced by lattice artefacts. Also, it is *a priori* not clear whether the interpolation of  $f_P\sqrt{M_P}$  between the results obtained in the static limit and the conventional approach is feasible at non-zero values of the lattice spacing. Since discretisation errors are potentially very different in the two approaches, a meaningful interpolation may only be possible after extrapolation to the continuum limit. We will return to this point in subsect. 3.4.

### 3.3. Results for pseudoscalar decay constants

We now compile and discuss the results for the pseudoscalar decay constants  $f_D$ ,  $f_B$ ,  $f_{D_s}$  and  $f_{B_s}$  from various authors and using different formulations of heavy quarks on the lattice.

#### 3.3.1. The conventional approach

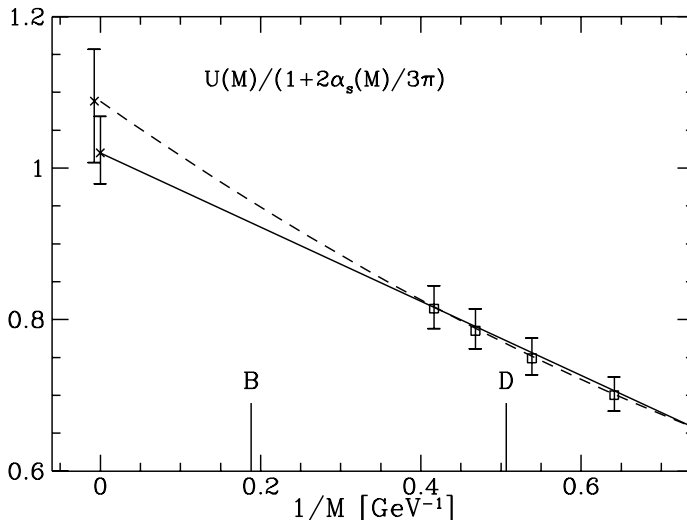


Fig. 2. Data for the quantity  $U(M)$  from the UKQCD collaboration<sup>101</sup>. The solid and dashed lines represent the linear and quadratic fits to the data. Radiative corrections to  $U(M)$  have been divided out.

We start with the decay constants  $f_D$  and  $f_{D_s}$ , which have only been calculated using the conventional (relativistic) formulation. The determination of  $f_D$  proceeds by interpolating the lattice data for  $\Phi(M_P)$  (c.f. eq. (64)) to the mass of the  $D$  meson, as either a linear or a quadratic function of  $1/M_P$ . In table 1 we list the results, also indicating the value of  $\beta$ , the normalisation of the quark fields and whether an improved action was used (i.e.  $c_{\text{sw}} > 0$ ). The first error on the decay constant is the statistical error, whereas the others are an estimate of systematic errors. The MILC collaboration<sup>110,111,112</sup> quote a third error which is an estimate of quenching effects, and which is obtained by comparing the results in the quenched approximation at  $a^{-1} \simeq 2$  GeV to a simulation with  $n_f = 2$  flavours of dynamical quarks at approximately the same value of  $a^{-1}$ .

Table 2 shows the corresponding results for  $f_B$  and  $f_{B_s}$ . Furthermore, the SU(3)-flavour breaking ratios  $f_{D_s}/f_D$  and  $f_{B_s}/f_B$  are listed in table 3. The extraction of  $f_B$  using the conventional method involves the extrapolation of  $\Phi(M_P)$  in  $1/M_P$  to the  $B$  system, which is an additional source of uncertainty. In order to have better control over this extrapolation, some authors prefer to interpolate between the values obtained in the static approximation and those from the conventional method<sup>99,102,110,111,112</sup>. As discussed in subsection 3.2, at a fixed value of  $\beta$  this appears only possible if either an improved action or the KLM norm is employed. Using instead the relativistic norm with  $c_{\text{sw}} = 0$  results in a flattening of  $\Phi(M_P)$  as  $M_P$  is increased, which is interpreted as a lattice artefact. This is consistent with the observation that early calculations using the conventional method obtained rather

Table 1. Results for  $f_D$  and  $f_{D_s}$  using the conventional formulation of heavy quarks. All values were obtained in the quenched approximation, except for those from the HEMCGC collaboration which were computed for  $n_f = 2$ . Infinite values of  $\beta$  symbolise results obtained after extrapolation to the continuum limit. Results by MILC and JLQCD are preliminary.

Collab.	$\beta$	$f_D$ [MeV]	$f_{D_s}$ [MeV]	norm	$c_{\text{sw}}$
APE <sup>120</sup>	6.2	221(17)	237(16)	rel.	1
MILC <sup>112</sup>	" $\infty$ "	196(9)(14)(8)	211(7)(25)(11)	KLM	0
JLQCD <sup>114,115</sup>	" $\infty$ "	202(8) $^{+24}_{-11}$	216(6) $^{+22}_{-15}$	KLM	0
LANL <sup>116,117</sup>	6.0	229(7) $^{+20}_{-16}$	260(4) $^{+27}_{-22}$	KLM	0
	" $\infty$ "	186(29)	218(15)	KLM	0
PCW <sup>102</sup>	" $\infty$ "	170(30)		KLM	0
PCW <sup>118</sup>	6.0	198(17)		rel.	0
HEMCGC <sup>121,122</sup>	5.6	200–287	220–320		0
	5.3	215(5)(40)(35)	287(5)(45)(40)	KLM	0
UKQCD <sup>101</sup>	6.2	185 $^{+4}_{-3}$ $^{+42}_{-7}$	212 $^{+4}_{-4}$ $^{+46}_{-7}$	rel.	1
	6.0	199 $^{+14}_{-15}$ $^{+27}_{-19}$	225 $^{+15}_{-15}$ $^{+30}_{-22}$	rel.	1
BLS <sup>99</sup>	6.3	208(9)(35)(12)	230(7)(30)(18)	KLM	0
ELC <sup>109</sup>	6.4	210(40)	230(50)	rel.	0
ELC <sup>124</sup>	6.2	181(27)		rel.	0
	6.0	197(14)		rel.	0
LDeG <sup>125</sup>	6.0	134(23)	157(11)	rel.	0
BDHS <sup>126</sup>	6.1	174(26)(46)	234(46)(55)	rel.	0

low values for  $f_D$  and  $f_B$  <sup>126,125</sup>, and underlines the importance of addressing the effects of large quark masses in the conventional approach.

In addition to using the KLM norm in conjunction with the otherwise unimproved Wilson action ( $c_{\text{sw}} = 0$ ), some collaborations <sup>99,110,111,112,115</sup> also include higher-order corrections for large quark mass, as explained in subsect. 2.2. The pseudoscalar meson mass  $M_P$  has been shifted accordingly, i.e.

$$M_P \rightarrow M'_P \equiv M_P + (\tilde{m}_2 - \tilde{m}_P), \quad (66)$$

where  $m_P$  and  $m_2$  are defined in eqs. (30) and (32), respectively, and also tadpole improvement has been applied to  $m_P$  and  $m_2$ . The mass dependence of  $\Phi(M_P)$  is then studied in terms of the shifted mass  $M'_P$ , which is the tree-level estimate of the kinetic mass appearing in the non-relativistic dispersion relation.

Tables 1 and 2 show that the results among different collaborations are broadly consistent, provided that the effects of large quark masses have been treated, either by employing an improved action, or by using the KLM norm. The error analyses by the different groups reveal that the statistical errors amount to 5–10%, so that the uncertainty in pseudoscalar decay constants is now dominated by systematic effects. In view of the large overall errors and the different treatment of the systematics, it would be premature to conclude on the basis of tables 1 and 2 that discretisation



Table 2. Results for  $f_B$  and  $f_{B_s}$  using the conventional formulation of heavy quarks. All values were obtained in the quenched approximation, except for those from the HEMCGC collaboration. Results by MILC and JLQCD are preliminary.

Collab.	$\beta$	$f_B$ [MeV]	$f_{B_s}$ [MeV]	norm	$c_{\text{sw}}$
APE <sup>120</sup>	6.2	180(32)	205(35)	rel.	1
MILC <sup>112</sup>	" $\infty$ "	166(11)(28)(18)	181(10)(36)(18)	KLM	0
JLQCD <sup>114,115</sup>	" $\infty$ "	179(11) $^{+2}_{-31}$	197(7) $^{+0}_{-35}$	KLM	0
PCW <sup>102</sup>	" $\infty$ "	180(30)		KLM	0
HEMCGC	5.6	152–235			0
<sup>121,122</sup>	5.3	150(10)(40)(40)		KLM	0
UKQCD <sup>101</sup>	6.2	160 $^{+6}_{-6}$ $^{+59}_{-19}$	194 $^{+6}_{-5}$ $^{+62}_{-9}$	rel.	1
	6.0	176 $^{+25}_{-24}$ $^{+33}_{-15}$		rel.	1
BLS <sup>99</sup>	6.3	187(10)(34)(15)	207(9)(34)(22)	KLM	0
ELC <sup>109</sup>	6.4	205(40)		rel.	0
BDHS <sup>126</sup>	6.1	105(17)(30)		rel.	0

Table 3. Results for the SU(3)-flavour breaking ratios  $f_{D_s}/f_D$  and  $f_{B_s}/f_B$  using the conventional formulation of heavy quarks. All values were obtained in the quenched approximation. Results by MILC are preliminary.

Collab.	$\beta$	$f_{D_s}/f_D$	$f_{B_s}/f_B$
APE <sup>120</sup>	6.2	1.07(4)	1.14(8)
MILC <sup>112</sup>	" $\infty$ "	1.09(2)(5)(5)	1.10(2)(5)(8)
LANL <sup>116,117</sup>	6.0	1.135(21) $^{+23}_{-6}$	
PCW <sup>102</sup>	" $\infty$ "	1.09(2)(5)	1.09(2)(5)
UKQCD <sup>101</sup>	6.2	1.18 $^{+2}_{-2}$	1.22 $^{+4}_{-3}$
	6.0	1.13 $^{+6}_{-7}$	1.17(12)
BLS <sup>99</sup>	6.3	1.11(6)	1.11(6)

errors are under control. This requires a detailed analysis of the continuum limit, which we shall attempt in the next subsection.

The ratios  $f_{D_s}/f_D$  and  $f_{B_s}/f_B$  listed in table 3 vary by about 10% among different groups, which is slightly larger than the typical statistical error. This is inspite of the fact that some of the systematic errors in these ratios (e.g. the renormalisation factor  $Z_A$ ) are expected to cancel, such that they are determined much more reliably.

Here we wish to make a few comments about the estimation of systematic errors. Most collaborations quote a systematic error coming from the uncertainty in the lattice scale. Apart from the statistical error in the quantity that is used to set the scale, this may also include the effects of choosing different quantities to estimate  $a^{-1}$  [GeV]. The MILC Collaboration<sup>112,113</sup> include this uncertainty in their estimation of quenching errors. Furthermore, MILC perform a detailed analysis of systematic errors after the extrapolation to the continuum limit. Their estimate

yields a total uncertainty in  $f_B$  due to using large quark masses of about 10% of the result. Further sizeable systematic effects are ascribed to the extrapolations in the lattice spacing and the light quark mass. By comparing results for  $f_B$  for  $n_f = 0$  and  $n_f = 2$  at similar values of  $a^{-1}$  [GeV], MILC conclude that  $f_B$  may be larger by around 10% in the unquenched theory.

Bhattacharya and Gupta<sup>116</sup> have analysed different prescriptions in the definition of the tadpole improved normalisation factor  $\tilde{Z}_A$ . Using either  $u_0 = \langle \frac{1}{3} \text{Re Tr } P \rangle$  or  $u_0 = 1/8\kappa_{\text{crit}}$  in eq. (45) leads to an uncertainty of 14 MeV in  $f_D$ , which is considered a conservative estimate by the authors. They also ascribe an error of around 5% to the uncertainty in fixing the charm mass, using either the kinetic mass  $M'_P$  or the conventional “pole” mass  $M_P$  for the heavy-light pseudoscalar meson. However, since only a single mass value for the heavy quark is used in<sup>116</sup>, the authors are not able to perform a detailed analysis of the mass behaviour, and thus the problem of using different definitions of heavy masses cannot be fully addressed in their study.

In fact, Allton *et al.*<sup>120</sup> have found that the mass dependence of  $\Phi(M_P)$  is only marginally changed by considering the “kinetic” mass instead of the “pole” mass. They quote their best estimates from their run at  $\beta = 6.2$ ,  $c_{\text{sw}} = 1$ , using results at  $\beta = 6.0$  as well as data with  $c_{\text{sw}} = 0$  to estimate systematic errors. Furthermore, Allton *et al.* emphasise that the data for  $\Phi(M_P)$  using  $c_{\text{sw}} = 1$  are indistinguishable from those for  $c_{\text{sw}} = 0$  computed with the KLM prescription, in good agreement with ref.<sup>101</sup> and this work (c.f. figure 1).

JLQCD investigate mass effects over a range of quark masses and lattice spacings using the unimproved Wilson action<sup>114,115</sup>. At fixed values of  $\beta$  they analyse the effects of using different field normalisations (relativistic or KLM) and definitions of the pseudoscalar mass (“pole” or “kinetic”). Whilst different prescriptions produce a fair amount of variation in the value of the decay constant at non-zero lattice spacing, JLQCD’s preliminary findings<sup>115</sup> indicate that these deviations are decreasing as  $a \rightarrow 0$ . Similar observations were made earlier by the PCW collaboration<sup>102</sup>.

### 3.3.2. *The static approximation*

Now we turn to the discussion of results for  $f_B$  obtained in the static approximation. In table 4 we list the results from several simulations. In general,  $f_B^{\text{stat}}$  turns out much larger than the results from the conventional approach. Especially some of the earlier simulations produced very large values<sup>118,133–135</sup>, which may partly be due to the fact that the axial current normalisation factor in the static approximation,  $Z_A^{\text{stat}}$ , was evaluated in bare perturbation theory, thus producing a much larger value.

In order to avoid discussing many different systematic effects in  $f_B^{\text{stat}}$  when comparing different simulations, we have also listed the matrix element  $A^L$  in lattice units in table 4 (see eq. (60)). By comparing results at fixed  $\beta$ , one observes consistency in  $A^L$  among many different collaborations over a wide range of  $\beta$  values. This is remarkable as even the use of an improved action for the light quark does not seem to have a discernible effect on  $A^L$  (see also the discussion in<sup>100</sup>). Thus,

whilst the numerical values for  $A^L$  obtained using either  $c_{\text{sw}} = 0$  or  $c_{\text{sw}} = 1$  are totally consistent at fixed  $\beta$ , the one-loop estimates of the renormalisation factor  $Z_A^{\text{stat}}$  are larger by 10–15% for  $c_{\text{sw}} = 1$  as compared to  $c_{\text{sw}} = 0$ . Therefore, as long as there is no non-perturbative determination of  $Z_A^{\text{stat}}$ , which may clarify the issue, lattice determinations of  $f_B^{\text{stat}}$  will always differ in the unimproved and improved theories at non-zero values of  $a$ . It is therefore of great importance to study the approach to the continuum limit of both cases.

As the signal-to-noise ratio in simulations of the static approximation is notoriously bad<sup>135,134</sup>, it is important to use an efficient smearing technique in order to extract a reliable signal. The most advanced calculations in the static approximation<sup>130,128,100</sup> use a variational approach in which a matrix correlator is constructed by computing cross correlations from different smearing functions. One can then diagonalise the matrix correlator and project onto the ground state, thereby eliminating approximately the contamination of the signal from higher excited states<sup>138</sup>.

Table 4. Results for  $f_B$ ,  $f_{B_s}/f_B$  and the matrix element in lattice units,  $a^{3/2}A^L$ , obtained in the static approximation. All data are from quenched simulations. The results in<sup>127</sup> are preliminary.

Collab.	$\beta$	$f_B^{\text{stat}}$ [MeV]	$f_{B_s}/f_B$	$a^{3/2}A^L$	$c_{\text{sw}}$
UKQCD <sup>100</sup>	6.2	266 <sup>+18</sup> <sub>-20</sub> <sup>+28</sup> <sub>-27</sub>	1.16 <sup>+4</sup> <sub>-3</sub>	0.112 <sup>+8</sup> <sub>-8</sub>	1
APE <sup>127</sup>	6.4	235(9)	1.13(2)	0.075(3)	1
	6.4	209(14)	1.12(7)	0.076(5)	0
	6.2	221(12)	1.12(7)	0.109(6)	1
	6.1	190(10)	1.13(5)	0.135(7)	0
	6.0	258(9)	1.19(3)	0.201(7)	1
FNAL <sup>128</sup>	“ $\infty$ ”	188(23)(15) <sup>+26</sup> <sub>-0</sub> (14)	1.22(4)(2)		0
	6.3	225(17)(14)	1.17(3)(1)	0.099(8)	0
	6.1	215(21)(14)	1.23(3)(2)	0.135(13)	0
	5.9	241(13)(13)	1.21(2)(1)	0.250(14)	0
	5.7	271(13)(20)	1.18(3)(1)	0.564(28)	0
APE <sup>129</sup>	6.2	290(15)(45)	1.11(3)	0.111(6)	1
UKQCD <sup>101</sup>	6.0	286 <sup>+8</sup> <sub>-10</sub> <sup>+67</sup> <sub>-42</sub>	1.13 <sup>+4</sup> <sub>-3</sub>	0.211 <sup>+6</sup> <sub>-7</sub>	1
BLS <sup>99</sup>	6.3	235(20)(21)	1.11(2)(2)	0.092(6)	0
Ken <sup>130,131</sup>	6.0	224 <sup>+9</sup> <sub>-7</sub>	1.22(1)	0.184(7)	0
SH <sup>132</sup>	6.0	297(36) <sup>+15</sup> <sub>-30</sub>		0.206(25)	0
APE <sup>133</sup>	6.0	370(40)	1.19(5)	0.22(2)	1
	6.0	350(40)(30)	1.14(4)	0.23(2)	0
PCW <sup>98</sup>	“ $\infty$ ”	230(22)(26)	1.16(5)		0
PCW <sup>118</sup>	6.0	366(22)(55)	1.10(9)		0
HS <sup>134</sup>	6.0	386(15)			0
ELC <sup>135</sup>	6.0	310(25)(50)		0.22(2)	0

A possible interpretation of the very low value for  $A^L$  observed by the Kentucky group<sup>130</sup>, who use a large basis of different smearing functions, is that there may be some residual contamination from higher excited states in the results of

Table 5. Results for  $f_B$  using NRQCD. The results by the SGO Collaboration<sup>105,106</sup> were obtained on dynamical configuration with  $n_f = 2$ .

Collab.	$\beta$	$a^{3/2}A^L$	$f_B$ [MeV]	$f_{B_s}/f_B$	$n_f$
SGO <sup>108</sup>	6.0		183(32)(28)(16)	1.17(7)	0
SGO <sup>106</sup>	5.6		126–166	1.24(4)(4)	2
Ken <sup>103</sup>	6.0	0.110 $^{+4}_{-5}$		1.15 $^{+2}_{-1}$	0
SH <sup>132</sup>	6.0	0.156(8)	171(22) $^{+19}_{-45}$		0

refs.<sup>135,133,98</sup>. This is not implausible, since typical values for the binding energy extracted from the exponential fall-off of the correlation function in eq.(58) are around  $\mathcal{E} \simeq 0.7$  in lattice units at  $\beta = 6.0$ . This is still rather large and thus great care is required in isolating the ground state. Therefore, despite using smeared sources, and in view of large overall statistical fluctuations, the results at the lower end of the range in  $\beta$  could still be affected by higher excited states if no variational approach is applied. The situation improves above  $\beta \geq 6.0$ , where the binding energies are lower such that not so much can be gained by employing variational smearing. At  $\beta = 6.2$ , UKQCD have explicitly verified that the contamination from higher states was negligible, and that their results with and without variational smearing were consistent<sup>100</sup>.

The dependence of  $f_B^{\text{stat}}$  on the number of dynamical quark flavours  $n_f$ , has been studied in refs.<sup>136,137</sup>. The results by the Rome2 group<sup>136</sup> indicate that at  $a^{-1} = 1.1 \text{ GeV}$  the value of  $f_B^{\text{stat}}$  increases by 15–20% for  $n_f = 3$ . Further calculations are clearly needed to confirm this sizeable flavour dependence.

### 3.3.3. *Non-relativistic QCD*

So far there are relatively few estimates of  $f_B$  using NRQCD. For all but one study<sup>108</sup>, an estimate for the axial current normalisation constant in NRQCD was not available, such that most previous studies had resorted to using  $Z_A^{\text{stat}}$ . The major results are listed in table 5. Quantities in which the current normalisation cancels, such as  $f_{B_s}/f_B$  are consistent with the results from the static approximation and the conventional approach.

A major advantage of NRQCD in studies of the scaling law for  $f_P\sqrt{M_P}$  is that it is possible to study the corrections in the inverse meson mass  $1/M$  starting from the static approximation as the limiting case. Indeed, very large  $1/M$  and  $1/M^2$  corrections to the scaling law eq.(62) have been observed in NRQCD<sup>104,105,106</sup>. However, as the NRQCD hamiltonian in those studies was obtained after truncation at order  $1/m_Q$  in the heavy quark mass, one may question the observation of large  $1/M^2$  corrections. More recent studies have therefore included all  $1/m_Q^2$  terms in the NRQCD action and operators. Preliminary results by Ali Khan and Bhattacharya<sup>107</sup> indicate that the individual corrections of  $1/M^2$  to the NRQCD hamiltonian amount to about 20% of the  $1/M$  corrections, although their effect on the slope of  $f_P\sqrt{M_P}$  is marginal, as the various  $1/m_Q^2$  corrections to the hamiltonian

and operators come in with opposite signs.

All of these findings must, however, be re-evaluated in the light of a recent study in which  $Z_A$  computed in NRQCD at one-loop order, has for the first time been applied. This has a dramatic effect on the  $1/M$  corrections to the scaling law, which turn out to be much smaller when  $Z_A$  is taken into account. Furthermore, the scale  $q^*$  at which the mean field improved coupling  $\alpha(q^*)$  in the one-loop expression for  $Z_A$  is evaluated (c.f. subsection 2.3) has a big influence on the mass behaviour of  $f_P\sqrt{M_P}$ . Choosing  $q^* = a^{-1}$ ,  $f_P\sqrt{M_P}$  is almost constant in  $1/M$ , whereas for  $q^* = \pi/a$  the slope of  $f_P\sqrt{M_P}$  in  $1/M$  is consistent with the findings using the conventional approach<sup>99,101</sup>. Performing a careful estimation of systematic errors, the authors of ref.<sup>108</sup> quote

$$f_B = 174(28)(26)(16) \text{ MeV}, \quad q^* = 1/a, \quad (67)$$

$$f_B = 183(32)(28)(16) \text{ MeV}, \quad q^* = \pi/a, \quad (68)$$

where the first error combines the statistical and the fitting error, the second comes from the uncertainty in the lattice scale, and the third is an estimate of uncertainties due to higher-order contributions to  $Z_A$  and neglected higher orders in  $1/M$ .

There are indications that consistency in the mass behaviour of  $f_P\sqrt{M_P}$  from the region of charm to the static limit is observed using different formalisms of treating heavy quarks on the lattice. It should, however, be emphasised that it is crucial to investigate the continuum limit of the mass dependence of  $f_P\sqrt{M_P}$ , which we will attempt in the next subsection.

### 3.4. The continuum limit

We are now in a position to study the continuum limit of heavy-light decay constants using results discussed in the previous subsection. Although some of the more recent simulations<sup>98,102,128,111,112,115</sup> have already performed an extrapolation to the continuum limit, we want to treat as many different results as possible on an equal footing and perform a thorough analysis of systematic errors in the final results.

As is apparent from tables 1–4, most results have been obtained for Wilson fermions with  $c_{\text{sw}} = 0$ . At present it is therefore not possible to perform the extrapolation  $a \rightarrow 0$  of the data with  $c_{\text{sw}} = 1$ , which would be an important consistency check. Furthermore, since the data of the MILC<sup>111,112</sup> and JLQCD<sup>115</sup> collaborations are still preliminary and are likely to be updated, we leave them out in the following analysis, despite their high statistics and large range in  $\beta$ .

Since the systematic effects in the results listed in tables 1–4 are quite different, e.g. the choice of lattice scale, the details of the quark field normalisation and in the evaluation of  $Z_A$ , a straightforward extrapolation of all listed results would be unreliable. Therefore, in order to study the mass dependence of  $f_P\sqrt{M_P}$  and obtain estimates for decay constants in the continuum, we adopt a similar strategy as described in<sup>23,102</sup>. The various steps of the procedure are as follows:

- (a) At a fixed value of  $\beta$  one forms the dimensionless ratio  $\Phi(M_P)/\sqrt{\sigma}^{3/2}$  using lattice data for  $\Phi(M_P)$  defined in eq. (64) and the string tension  $\sqrt{\sigma}$ .
- (b) The ratio  $\Phi(M_P)/\sqrt{\sigma}^{3/2}$  is then interpolated to common values of  $M_P/\sqrt{\sigma}$ .
- (c) At every fixed value of  $M_P/\sqrt{\sigma}$  one extrapolates  $\Phi(M_P)/\sqrt{\sigma}^{3/2}$  to the continuum limit as a function of  $a\sqrt{\sigma}$ .
- (d) Now one sets the scale using extrapolated lattice data for, e.g. the pion decay constant,  $f_\pi/\sqrt{\sigma}|_{a=0}$  of the  $\rho$  meson mass  $M_\rho/\sqrt{\sigma}|_{a=0}$ . The continuum value of  $\Phi(M_P)/\sqrt{\sigma}^{3/2}$  is interpolated to the desired value of the heavy-light meson mass, and finally one converts back to the decay constant in physical units using the definition of  $\Phi(M_P)$ .

This procedure implies that in step (d)  $f_B$  is obtained through an interpolation between the result in the static approximation and those using relativistic heavy quarks. Therefore, a separate extrapolation of the data for  $f_B^{\text{stat}}$  is required (i.e. step (c) for  $\sqrt{\sigma}/M_P = 0$ ).

The difference between this procedure and the extrapolations performed in refs. <sup>128,112,115</sup> is that in the latter the conversion of heavy-light decay constants into physical units precedes the extrapolation to  $a = 0$ . This is feasible if the scale is measured as well at every value of  $\beta$  considered. The universal treatment of a number of different simulations, however, forces one to use the extrapolated lattice scales, since the values of  $\beta$  at which the quantity to set the scale is measured do not necessarily coincide with the  $\beta$  values used in the computation of heavy-light decay constants.

Lattice data for the string tension  $a\sqrt{\sigma}$  used in the following extrapolations are listed in appendix B. In order to perform a controlled extrapolation to the continuum limit of a number of hadronic quantities, it has been suggested <sup>45</sup> that the hadronic scale  $r_0$  is to be preferred over the string tension  $\sqrt{\sigma}$ . However, despite the merits of choosing  $r_0$  to monitor the approach of the continuum limit, it has so far only been determined in a fairly limited range of  $\beta$  (see refs. <sup>195–198,202</sup>). Therefore we stick to the string tension for our purposes.

Appendix B also describes the details of the continuum extrapolation of quantities in the light quark sector, such as  $f_\pi$ ,  $M_\rho$  and the 1P–1S splitting in charmonium,  $\Delta_{1\text{P–1S}}$ . The pion decay constant  $f_\pi$  is widely used to set the scale, because both  $f_\pi$  and the heavy-light decay constant  $f_P$  are subjected to similar systematic errors – at least in the conventional approach – such as quenching errors and uncertainties in  $Z_A$ . It can therefore be expected that some of these effects cancel if the conversion is performed using  $f_\pi$ . In ref. <sup>203</sup> it was argued that the 1P–1S splitting in charmonium is largely insensitive to lattice artefacts, which also makes it a reliable quantity to set the scale. The mass of the  $\rho$  meson, on the other hand, shows a strong dependence on the lattice spacing for unimproved Wilson fermions (see e.g. refs. <sup>23</sup>, such that it is not clear *a priori* whether or not one controls its extrapo-

lation to the continuum limit well enough. We include the mass of the  $\rho$  meson nevertheless in this study.

In this review we choose to quote our best estimates using  $f_\pi$  to set the scale. Systematic errors are estimated by varying

- the details in the evaluations of  $Z_A$  and  $Z_A^{\text{stat}}$
- the field normalisation of propagating heavy quarks (KLM or relativistic)
- the quantity that sets the scale
- the minimum value  $\beta_{\text{min}}$  which is used in the extrapolation in step (c) above (i.e. the maximum value of  $a$  [fm])

### 3.4.1. Extrapolation of the data obtained in the static approximation

We start our analysis by considering extrapolations of  $f_B^{\text{stat}}$  for  $c_{\text{sw}} = 0$ , using the tadpole improved value for  $Z_A^{\text{stat}}$  (see appendix A). In figure 3 we have plotted the ratio  $f_B \sqrt{M_B} |^{\text{stat}} / \sqrt{\sigma}^{3/2}$  as a function of the string tension in lattice units. Taking the data from refs. <sup>98,99,127,128,130,132,133,135</sup>, it can be seen from the figure that the simultaneous extrapolation of all data is not feasible and results in a large value of  $\chi^2/\text{dof}$ . We have therefore chosen to divide the data sample into two sets that each can be extrapolated with acceptable  $\chi^2/\text{dof}$ . Combining the data from refs. <sup>99,127,128,130,132</sup> into “set 1” and those from refs. <sup>98,132,133,135</sup> into “set 2”, we note that the values in set 2 are in general higher than those in set 1. As discussed in the previous subsection, a possible explanation for this may be the presence of residual contamination from excited states, because no variational smearing was used in set 2. However, since it is impossible at this stage to further investigate the apparent discrepancies between sets 1 and 2, we will take set 1 for our best estimate for  $f_B^{\text{stat}}$ , whilst quoting the extrapolated value from set 2 as a systematic error.

We now discuss the dependence on the minimal  $\beta$  value,  $\beta_{\text{min}}$ , used in the extrapolation. Figure 3 shows that the extrapolated result for  $f_B \sqrt{M_B} |^{\text{stat}} / \sqrt{\sigma}^{3/2}$  from set 1 changes if the point at  $\beta = 5.7$  is included or not. This may signal that higher corrections in the lattice spacing may be important if one includes data for which  $a$  can be as large as 0.17 fm. This observation is consistent with the findings of ref. <sup>139</sup>, where it was concluded that the expected scaling behaviour of the quantity  $A^L$  is observed down to values of  $\beta \simeq 5.9 - 6.0$ . However, since one obtains a perfectly good fit of set 1 if the result at  $\beta = 5.7$  is included, we again quote the difference between results obtained for  $\beta_{\text{min}} = 5.7$  and  $\beta_{\text{min}} = 5.9$  as a systematic error.

Our best estimate is computed for  $\beta_{\text{min}} = 5.9$  and we obtain

$$\frac{f_B \sqrt{M_B} |^{\text{stat}}}{\sqrt{\sigma}^{3/2}} = 1.81 \pm 0.16 (\text{stat}) {}^{+0.31}_{-0.20} (\text{extr}) \pm 0.07 (\text{norm}), \quad (69)$$

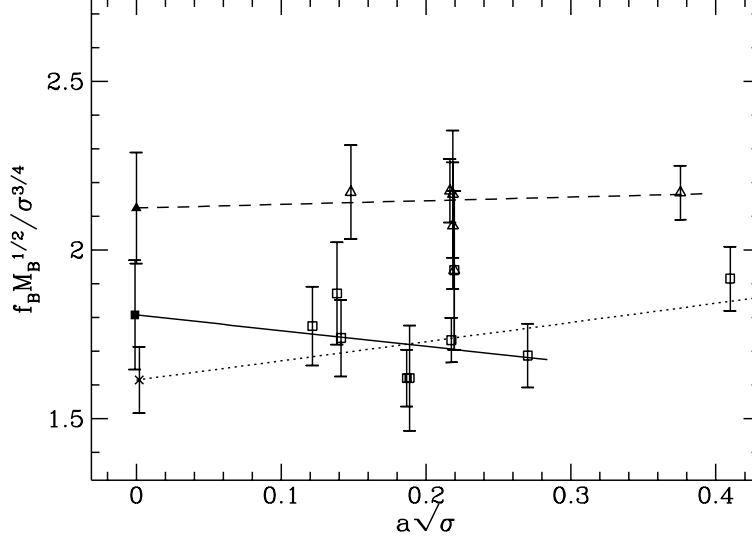


Fig. 3. The ratio  $f_B \sqrt{M_B} |^{\text{static}} / \sqrt{\sigma}^{3/2}$  for  $c_{\text{sw}} = 0$  plotted versus the string tension. Open squares denote the results from refs. 128,127,99,130,132,133,98,135 (“set 1”), whereas open triangles represent refs. 98,133,135,132 (“set 2”). The solid line represents the linear extrapolation of the data in set 1 for  $\beta_{\min} = 5.9$ , the dotted line is the extrapolation of set 1 for  $\beta_{\min} = 5.7$ , and the dashed curve denotes the extrapolation of the data in set 2. The tadpole improved normalisation factor of the axial current,  $Z_A^{\text{stat}}$  was used.

where the first error is statistical, the second arises from the difference between sets 1 and 2 as well as using  $\beta_{\min} = 5.7$ . The third error is due to the variations from using different prescriptions in the numerical evaluation of  $Z_A^{\text{stat}}$ .

Using  $f_\pi / \sqrt{\sigma}|_{a=0} = 0.285(13)$  from the extrapolation of the data of the GF11 collaboration<sup>205</sup> (see appendix B) and  $f_\pi = 131$  MeV to convert into physical units, we find

$$f_B^{\text{stat}} = 245 \pm 27 \text{ (stat)} \quad {}^{+42}_{-39} \text{ (syst) MeV}, \quad (70)$$

where we have combined different systematic errors in quadrature, including those from using  $M_\rho$  and  $\Delta_{1P-1S}$  to set the scale. Given the large errors, this result is not incompatible with the fairly low result quoted by the FNAL group<sup>128</sup> and that of the PCW collaboration<sup>98</sup> (see table 4). It should be noted, however, that the result in eq. (70) is a consequence of omitting the results at low  $\beta$  (i.e.  $\beta = 5.7$ ) in the extrapolation. If those data are included one obtains the lower value of  $f_B^{\text{stat}} = 218 \pm 20 \text{ (stat) MeV}$ .

### 3.4.2. Extrapolation of data using relativistic heavy quarks

Now we proceed to discuss the extrapolation of heavy-light decay constants using the conventional approach. This will finally enable us to study the scaling law for  $f_P \sqrt{M_P}$ , eq. (62) in the continuum limit.



In order to be able to interpolate  $f_P\sqrt{M_P}$  to common values of  $M_P$  whilst comparing the use of the kinetic versus the pole mass, we need to resort to data whose mass dependence has been published (as a function of the hopping parameter of the heavy quark). Therefore we only use refs. <sup>99,102,109,116,119</sup>, leaving the data by MILC <sup>111,112</sup> and JLQCD <sup>114,115</sup> to be included in the future. Furthermore we chose not to use the data of ref. <sup>109</sup>. As already noted in <sup>23</sup>, it is questionable whether the asymptotic behaviour of the relevant correlation functions has been reached in <sup>109</sup>, since no smearing has been applied in the computation of the relevant correlation functions. Failure to isolate the ground state leads to an overestimate of the matrix element which is used to extract  $f_P$ . In fact, the quantity  $\Phi(M_P)$  from ref. <sup>109</sup> is very different compared to refs. <sup>99,102,116,119</sup> when all data are scaled appropriately and treated equally. Also some of the very early calculations <sup>124,125,126</sup> did not apply smearing techniques to improve the isolation of the ground state, and consequently we do not include them in our analysis.

The data for  $f_P\sqrt{M_P}$  are used to compute  $\Phi(M_P)/\sqrt{\sigma}^{3/2}$ , which is then interpolated to fixed values of  $\sqrt{\sigma}/M_P$  between 0.12 and 0.29, corresponding to heavy-light meson masses of 1.4–3.5 GeV. In ref. <sup>116</sup> only a single value of the heavy quark mass was considered, which corresponds to an inverse pole mass of  $\sqrt{\sigma}/M_P \simeq 0.283$  or to  $\sqrt{\sigma}/M'_P \simeq 0.260$  if the definition of the kinetic mass, eq. (66), is used. Only at these values of the inverse pole and kinetic masses, respectively could the results of ref. <sup>116</sup> be included in the extrapolation to the continuum limit.

In order to test the stability of the extrapolations at fixed  $\sqrt{\sigma}/M_P$ , we compare four procedures for which different evaluations of  $Z_A$  and different concepts to deal with heavy mass effects are compared:

- (1) KLM norm, kinetic mass, tadpole improved  $Z_A$
- (2) KLM norm, pole mass, tadpole improved  $Z_A$
- (3) relativistic norm, pole mass, tadpole improved  $Z_A$
- (4) relativistic norm, pole mass,  $Z_A$  in boosted perturbation theory

Here, the kinetic mass is always evaluated using eq. (66), in contrast to some results in refs. <sup>115,106</sup> where the kinetic mass was extracted from the measured dispersion relation. It should be mentioned at this point that using the KLM norm together with the pole mass may, after all, be an ill-defined concept as large mass corrections are only addressed at leading order, thus resulting in an incomplete treatment of these effects. In figure 4 we plot the extrapolation of  $\Phi(M_P)$  to  $a = 0$  for all four schemes listed above. A remarkable feature is that for  $\sqrt{\sigma}/M_P > 0.21$ , the results in the continuum limit are rather consistent, including the data computed using the KLM norm in conjunction with the pole mass. Since at fixed  $\beta$  the data computed using the relativistic norm show the wrong qualitative behaviour (see figure 1), this is quite a surprising result. Thus, at this stage it appears that the details of the procedure employed to deal with large mass effects and the normalisation

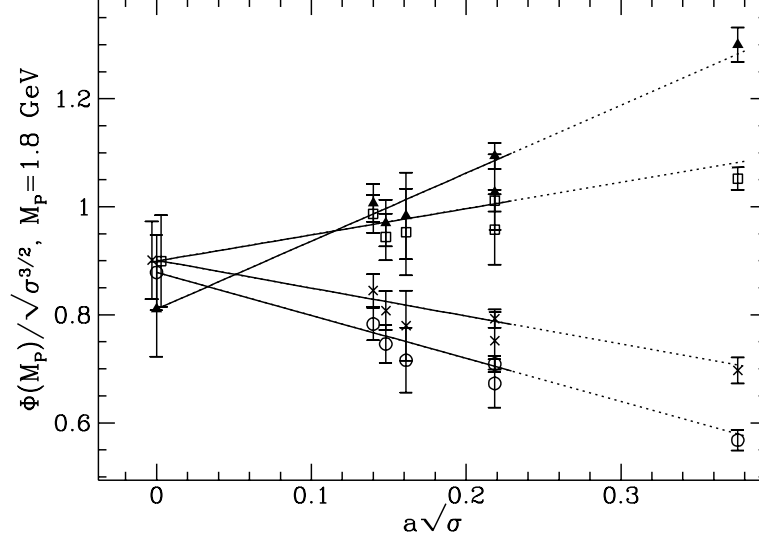


Fig. 4. The quantity  $\Phi(M_P)/\sqrt{\sigma^{3/2}}$  plotted as a function of the string tension in lattice units. Open squares represent the data computed procedure (1) as described in the text. Full triangles correspond to procedure (2), and the crosses and open circles represent the data using procedures (3) and (4), respectively. The solid lines denote the linear extrapolations of  $\Phi(M_P)/\sqrt{\sigma^{3/2}}$  to the continuum limit, using only the data for which  $\beta \geq 6.0$ . The dotted lines are the continuation of the fits to the point at  $\beta = 5.74$ .

factor  $Z_A$  produce a variation of only 3–5% in the continuum results for  $\Phi(M_P)$  for meson masses  $M_P \lesssim 2.2$  GeV. These observations are consistent with the findings in refs. <sup>102,115</sup>. However, the spread of results at  $a = 0$  using different procedures increases for larger masses, as can be seen in figure 5. This is an indication that eventually lattice artefacts make the continuum extrapolation harder to control if the quark mass is chosen very large. The slope of  $\Phi(M_P)/\sqrt{\sigma^{3/2}}$  as a function of  $a\sqrt{\sigma}$  increases for larger heavy quark mass, which is the expected behaviour as the influence of lattice artefacts becomes greater. As figure 4 shows, the results computed using the KLM norm and the kinetic mass show the smallest slope in the lattice spacing  $a$  compared to all other procedures employed. Unlike in the case of the static approximation, the extrapolations of  $\Phi(M_P)/\sqrt{\sigma^{3/2}}$  for relativistic heavy quarks are fairly insensitive to the value of  $\beta_{\min}$ . This can be seen from figure 4 where the data for  $\Phi(M_P)/\sqrt{\sigma^{3/2}}$  at  $\beta = 5.74$  are not incompatible with the extrapolations performed for  $\beta_{\min} = 6.0$ . However, below we will still use  $\beta_{\min} = 6.0$  for our best estimates as a safeguard against lattice effects in the final results, especially since the lattice spacing at  $\beta = 5.74$  is only  $a^{-1} \simeq 1.1$  GeV.

### 3.4.3. Interpolation to the physical meson masses

We are now in a position to perform step (d) and interpolate  $\Phi(M_P)/\sqrt{\sigma^{3/2}}$

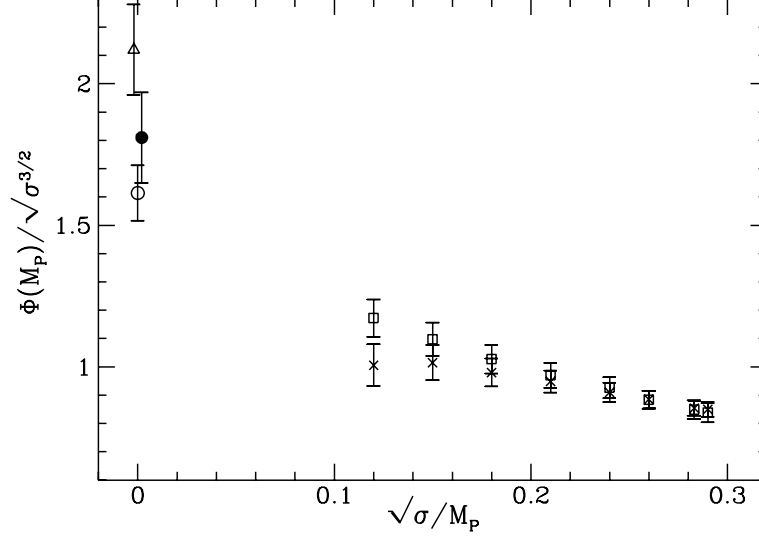


Fig. 5. The quantity  $\Phi(M_P)/\sqrt{\sigma}^{3/2}$  in the continuum limit as a function of  $\sqrt{\sigma}/M_P$ . Open squares denote the data computed using procedure (1), whereas the crosses represent the points obtained using procedure (3). Both sets were obtained using  $\beta_{\min} = 5.7$  in the extrapolation. For  $\Phi(M_P)/\sqrt{\sigma}^{3/2}$  in the static approximation, the circles denote the extrapolated values for set 1 using  $\beta_{\min} = 5.7$  (open symbol) and  $\beta_{\min} = 5.9$  (full symbol). The value obtained using set 2 is denoted by the triangle.

to the physical meson masses. Setting the scale by  $f_\pi/\sqrt{\sigma}|_{a=0} = 0.285(13)$ , we have interpolated our results for  $\Phi(M_P)/\sqrt{\sigma}^{3/2}$  at  $\sqrt{\sigma}/M_P = 0.21, 0.24$  and  $0.26$  to  $\sqrt{\sigma}/M_D = 0.245(11)$ . Our final result for  $f_D$  thus is

$$f_D = 191 \pm 19 \text{ (stat)} \pm 3 \text{ (extr)} \pm 0 \text{ (scale)} \text{ MeV}, \quad (71)$$

where the first error is statistical, the second is an estimate of systematic effects by varying  $\beta_{\min}$  and the treatment of large mass effects. The third error is due to choosing  $M_\rho$  or  $\Delta_{1P-1S}$  to set the scale. The latter effect is predominantly due to the known mismatch of  $f_\pi/M_\rho$  computed in the quenched approximation and the experimental result, which is partly ascribed to quenching.

In the case that the light quark has been interpolated to the mass of the strange quark, steps (a)–(d) of the extrapolation procedure are entirely analogous, and for  $f_{D_s}$  we obtain

$$f_{D_s} = 206 \pm 17 \text{ (stat)} \pm 6 \text{ (extr)} \pm 0 \text{ (scale)} \text{ MeV}. \quad (72)$$

By interpolation of the data for  $\Phi(M_P)/\sqrt{\sigma}^{3/2}$  between the points in the static approximation and those at finite mass  $M_P$  to the mass of the  $B$  meson we obtain an estimate for  $f_B$ . Here, however, there are two more sources of systematic errors which we include in our final result. The first is the variation on  $f_B\sqrt{M_B}$  in the

static approximation by using set 2 instead of set 1 for the central value. The second arises by choosing different sets of values for  $\sqrt{\sigma}/M_P$  that are included in the interpolation. Our best estimate is obtained using set 1 and  $\sqrt{\sigma}/M_P = 0.21, 0.24$  and  $0.26$  as in the case of  $f_D$ . Our result for  $f_B$  is

$$f_B = 172 \pm 24 \text{ (stat)} \quad {}^{+13}_{-12} \text{ (fits)} \quad {}^{+0}_{-15} \text{ (scale)} \text{ MeV}. \quad (73)$$

We can now analyse the mass behaviour of  $\Phi(M_P)/\sqrt{\sigma}^{3/2}$  in the continuum limit and deduce the leading correction in  $1/M_P$  to the scaling law eq. (62). Figure 5 is the analogue of figure 1 at zero lattice spacing. If we parametrise  $\Phi(M_P)$  as

$$\Phi(M_P) = \Phi(M_P)_\infty \left( 1 + \frac{C}{M_P} + \frac{D}{M_P^2} \right) \quad (74)$$

we obtain  $C = 0.9 - 2.0 \text{ GeV}$ . Thus, the conclusions reached at finite values of  $a$  are also valid in the continuum limit. The large uncertainty in  $C$  is partly due to the variation of  $\Phi(M_P)/\sqrt{\sigma}^{3/2}$  under changes in  $\beta_{\min}$ , and in particular to using either set 1 or set 2 in the interpolation to the mass of the  $B$  meson (the highest values for  $C$  are obtained by using set 2 in the static approximation).

The ratios  $f_{D_s}/f_D$  and  $f_{B_s}/f_B$  are also of great interest. Since it can be expected that systematic effects cancel partially in these ratios, one can attempt a straightforward extrapolation of the results quoted in refs. <sup>99,102,112,113,116</sup> and refs. <sup>98,99,127,128,130</sup> for  $f_{B_s}/f_B$  in the static approximation. In figure 6 we have plotted these extrapolations as a function of  $a\sqrt{\sigma}$ , and one can see that the results show a fairly flat behaviour as the continuum limit is approached. For our final results at  $a = 0$  we have again chosen  $\beta_{\min} = 6.0$  and continued the fits to lower values of  $\beta$  in figure 6 for illustrative purposes. We obtain

$$\frac{f_{D_s}}{f_D} = 1.08(8), \quad \frac{f_{B_s}}{f_B} = 1.14(8) \quad (75)$$

$$\left. \frac{f_{B_s}}{f_B} \right|_{\text{stat}} = 1.07(5) \quad {}^{+12}_{-0}, \quad (76)$$

where we have used set 1 for the extrapolation of  $f_{B_s}/f_B$  in the static approximation. If instead one computes the ratio  $f_{D_s}/f_D$  using our estimates in eqs. (71), (72) one obtains  $f_{D_s}/f_D = 1.08(14) \quad {}^{+1}_{-0}$  in very good agreement with the above result, albeit with a larger error.

### 3.5. Summary and comparison

The analysis of lattice results for heavy-light decay constants shows that essentially a consistent picture emerges from all three methods of simulating heavy quarks. The errors are, however, still fairly large, so that this statement has to be monitored as more precise lattice data become available. Adding all errors in quadrature, our best estimates for the decay constants  $f_D$ ,  $f_{D_s}$ ,  $f_B$ ,  $f_{B_s}$  and  $f_B^{\text{stat}}$  are listed in tables 6 and 7.

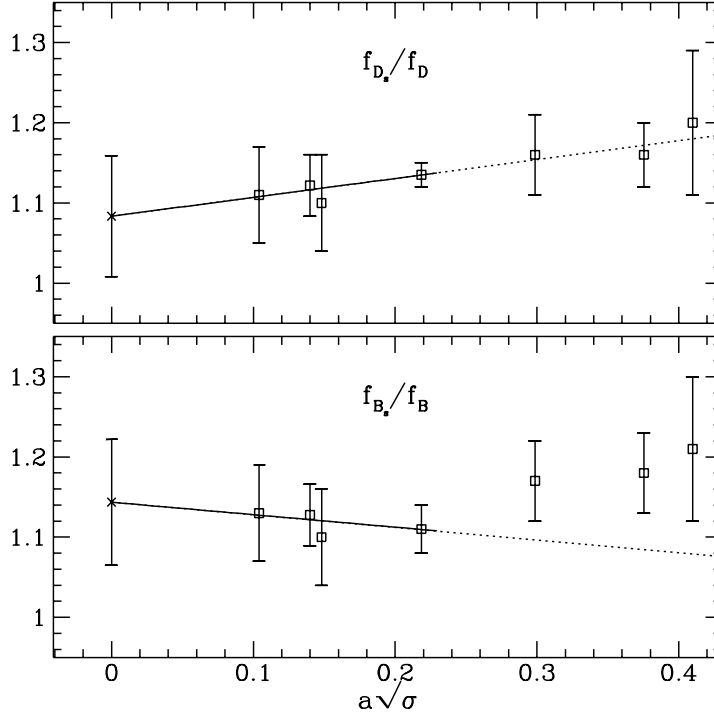


Fig. 6. Extrapolations of  $f_{B_s}/f_B$  and  $f_{D_s}/f_D$  to the continuum limit as a function of the string tension. The dotted lines are the continuations of the fits performed for  $\beta \geq 6.0$ . Data at common values of  $a\sqrt{\sigma}$  have been combined in a weighted average.

The large  $1/M$  corrections to the scaling law for  $f_P\sqrt{M_P}$  are now firmly established. In particular, the behaviour is not changed in the continuum limit. Furthermore, the heavy quark spin symmetry is manifest in the infinite mass limit, as  $U(M)$ , the ratio of matrix elements of the axial and vector currents indeed approaches unity. Also for this quantity the corrections in  $1/M$  at the  $B$  and  $D$  meson masses are sizeable.

The continuum limit requires further investigation. In particular it is necessary to increase the reliability of the extrapolations by going to smaller values of the lattice spacing, which correspond to  $\beta$  values larger than 6.3. Furthermore, as an important check against the influence of lattice artefacts more data using improved actions and operators need to be computed in the range  $\beta \geq 6.0$ , in order to allow for a separate continuum extrapolation. So far, quite a number of results quoted at non-zero lattice spacing are in agreement with the continuum result derived in this analysis (c.f. tables 1 and 2). In view of the large errors, however, this should not be taken as evidence that the continuum limit has essentially been reached already.

We can now compare continuum lattice results for heavy-light decay constants (also using the values quoted in other recent global analyses of lattice data<sup>18,23,25,26</sup>) to the findings of other theoretical methods and experimental results. In tables 6

Table 6. Summary of results for decay constants of charmed mesons.

Source	Author	$f_D$ [MeV]	$f_{D_s}$ [MeV]	$f_{D_s}/f_D$
Lattice	This work	$191^{+19}_{-28}$	$206^{+18}_{-28}$	1.08(8)
	Martinelli <sup>25</sup> , Flynn <sup>18,26</sup>	205(15)	235(15)	1.15(5)
	Sommer <sup>23</sup>	164(20)		
Sum	Neubert <sup>140</sup>	170(30)		
Rules	Dominguez <sup>143</sup>	139 – 234	174 – 269	1.21(6)
	Narison <sup>144,146</sup>	171(16)	197(20)	1.15(4)
Quark Models	Capstick+Godfrey <sup>156</sup>	240(20)	290(20)	1.21(13)
	Oakes <sup>157</sup>			0.985
	Hwang+Kim <sup>158</sup>	253(65)	265(68)	1.045
	Hwang+Kim <sup>159</sup>			1.201
Exp.	Average <sup>149,150</sup>	< 310	241(21)(30)	
	L3 <sup>155</sup>		309(58)(33)(38)	

and 7 we compare our best estimates with those from QCD sum rules, potential models and experimental results where available. The tables highlight the large uncertainties which are present in all determinations of these quantities so far. As mentioned before, lattice results suffer from systematic effects due to quenching, uncertainties in the extrapolation procedure and the treatment of heavy quarks. Estimates obtained using QCD sum rules are rather sensitive to the choice of input parameters in the evaluation, which in the past has sparked a long controversy among different authors. More recent results from the sum rule approach<sup>140–143,146,147</sup>, however, agree quite well with those obtained on the lattice. It should be noted that QCD sum rule estimates for  $f_{P_s}/f_P$  are somewhat larger than the lattice values. It is, however, difficult to estimate the real uncertainties associated with the results obtained using QCD sum rules. An interesting result is quoted in ref.<sup>160</sup>, where an upper bound on  $f_B$ , i.e.  $f_B < 195$  MeV is derived in a model-independent way, using rigorous QCD dispersion relations.

Heavy-light decay constants are hard to measure experimentally, since the leptonic width is small compared to the total width, and also because the presence of a neutrino in the final state complicates the analysis. Furthermore, the leptonic decay rate for a  $B$  meson is Cabibbo-suppressed, since it is proportional to  $|V_{ub}|^2$ , which puts it beyond the reach of current experiments. For charmed mesons, only an upper bound can be quoted for  $f_D$ <sup>149</sup> (c.f. table 6), whereas leptonic decays of  $D_s$  are Cabibbo favoured, since their rate is proportional to  $|V_{cs}|^2$ . Thus,  $f_{D_s}$  has indeed been measured by several experiments<sup>150–155</sup>.

The observation of large  $1/M$  corrections to eq. (62) in lattice calculations has been confirmed by QCD sum rules<sup>140–142,144,145,148</sup>. Sum rule estimates for the coefficient  $C$  in eq. (74) vary in the range 0.7–1.3 GeV, in good agreement with the lattice result quoted in subsection 3.4. So far, only lattice calculations using NRQCD without the axial current normalisation have produced substantially larger

Table 7. Summary of results for decay constants of bottom mesons.

Source	Author	$f_B$ [MeV]	$f_B^{\text{stat}}$ [MeV]	$f_{B_s}/f_B$
Lattice	This work	$172^{+27}_{-31}$	$245^{+50}_{-47}$	1.14(8)
	Martinelli <sup>25</sup> , Flynn <sup>18,26</sup>	175(25)		1.15(5)
	Sommer <sup>23</sup>	180(46)	276(37)	1.10 – 1.18
Sum	Neubert <sup>140</sup>	190(50)	200 – 300	
Rules	Eletsii+Shuryak <sup>141</sup>	150 – 175	165 – 200	
	Bagan <i>et al.</i> <sup>142</sup>		195 – 245	
	Dominguez <sup>143</sup>	133 – 183		1.22(2)
	Narison <sup>144,146</sup>	209(34)	259(41)	1.16(4)
Quark Models	Capstick+Godfrey <sup>156</sup>	155(15)		1.35(18)
	Oakes <sup>157</sup>			0.989
	Hwang+Kim <sup>158</sup>	201(51)		1.053
	Hwang+Kim <sup>159</sup>			1.173
QCD DR	Boyd <i>et al.</i> <sup>160</sup>	< 195		

corrections, such as  $C = 2.8(5)$  GeV quoted in ref.<sup>106</sup>.

To summarise, we have shown that lattice calculations using unimproved conventional and static heavy quarks have produced results for heavy-light decay constants with a total accuracy of 15% for charmed and 30% for bottom mesons. A number of systematic errors necessitate further studies, as signified by the rather large errors. Preliminary results from runs with dynamical quarks<sup>112,136</sup> suggest that decay constants could increase by up to 10% in the unquenched theory. However, unlike some time ago, there is now agreement between lattice calculations and QCD sum rules, and also the few experimental results. It is of great importance to increase the precision of lattice data, especially in view of future dedicated experiments for  $B$  physics.

#### 4. $B^0-\overline{B}^0$ Mixing

We will now turn the discussion to lattice calculations of the  $B$  parameter  $B_B$ , which is relevant for  $B^0-\overline{B}^0$  mixing. The lattice estimates for  $B_B$  and the decay constant  $f_B$  from the previous section can then be combined into the quantity  $f_B\sqrt{B_B}$ , which is of particular interest, since it constrains the possible values of the parameters  $\rho$  and  $\eta$  in the standard Wolfenstein parametrisation of the CKM matrix. At the end of this section, we will therefore attempt to quote a common estimate for this quantity using data from several lattice calculations and study its phenomenological implications in section 5.

##### 4.1. The $\Delta B = 2$ four-fermion operator on the lattice

In the continuum the interpolating operator for oscillations between a  $B^0$  and a

$\overline{B}^0$  meson is the four-fermion operator  $O_L$  defined by

$$O_L = (\bar{b}\gamma_\mu(1 - \gamma_5)q) (\bar{b}\gamma_\mu(1 - \gamma_5)q). \quad (77)$$

This operator enters the  $\Delta B = 2$  effective Hamiltonian<sup>161</sup>. The amplitude of  $B^0 - \overline{B}^0$  mixing is usually expressed in terms of the  $B$  parameter, which is the ratio of the operator matrix element to its value in the so-called vacuum insertion approximation

$$B_B(\mu) \equiv \frac{\langle \overline{B}^0 | O_L(\mu) | B^0 \rangle}{\frac{8}{3} |\langle 0 | A_4 | B^0 \rangle|^2} = \frac{\langle \overline{B}^0 | O_L(\mu) | B^0 \rangle}{\frac{8}{3} f_B^2 M_B^2}. \quad (78)$$

Here,  $\mu$  is a renormalisation scale, and  $A_4$  is the temporal component of the heavy-light axial current  $A_\mu = \bar{b}\gamma_\mu\gamma_5q$ . The dependence of  $B_B$  on the renormalisation scale can be removed by multiplication with a factor derived from the anomalous dimension of  $O_L$ . At leading order (LO) or next-to-leading order (NLO) respectively, a renormalisation group invariant  $B$  parameter can be defined by

$$\hat{B}_B^{\text{LO}} = \alpha_s(\mu)^{-2/\beta_0} B_B(\mu) \quad (79)$$

$$\hat{B}_B^{\text{NLO}} = \alpha_s(\mu)^{-2/\beta_0} \left( 1 + \frac{\alpha_s(\mu)}{4\pi} J_{n_f} \right) B_B(\mu), \quad (80)$$

where  $\beta_0 = 11 - 2n_f/3$  and  $J_{n_f}$  is derived from the one- and two-loop anomalous dimensions  $\gamma_L^{(0)}$  and  $\gamma_L^{(1)}$  of the operator  $O_L$ . In the  $\overline{\text{MS}}$  scheme one obtains<sup>161</sup>

$$J_{n_f} = \frac{1}{2\beta_0} \left( \gamma_L^{(0)} \frac{\beta_1}{\beta_0} - \gamma_L^{(1)} \right), \quad \beta_1 = 102 - \frac{38}{3}n_f, \quad (81)$$

$$\gamma_L^{(0)} = 4, \quad \gamma_L^{(1)} = -7 + \frac{4}{9}n_f. \quad (82)$$

With these definitions  $\hat{B}_B$  is renormalisation group invariant only up to leading order and next-to-leading order, respectively.

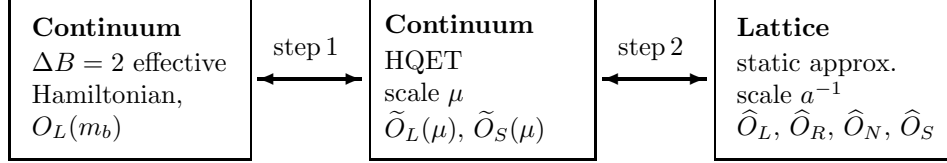
If the operator matrix element is evaluated on the lattice using Wilson fermions, the contributions of the corresponding operators with opposite and mixed chirality need also to be taken into account, as was explained in subsection 2.3. Since every operator has to be renormalised separately, the matching between the lattice operators and their continuum counterparts is potentially an intricate problem. Hence, in the case of four-fermion operators, the importance of a non-perturbative determination of the various matching factors is even greater. Attempts in this direction have been reported in the context of the  $B$  parameter  $B_K$ <sup>84,85</sup>.

Lattice results for the  $B$  parameter  $B_B$  have been published recently using the static approximation<sup>100,162,163</sup> and also propagating heavy quarks<sup>114,164,165</sup>. Earlier attempts are discussed in refs.<sup>109,126,135</sup>.

Here we shall describe in some detail the evaluation of  $B_B$  in the static approximation and the subsequent matching of the results in the effective lattice theory to the  $\Delta B = 2$  Hamiltonian in the continuum, which plays the rôle of the “full” theory, even though it is an effective theory in itself. The matching is usually performed in two steps (although there is in principle no need to do so), in which one



first matches the operator in full QCD at scale  $\mu = m_b$  to the continuum effective theory (i.e. HQET). In the second step one matches the basis of local operators in the continuum effective theory to those in the effective theory on the lattice. The following diagram illustrates the two-step process and lists the operators and renormalisation scales at every stage:



Thus, when relating the continuum full theory to the continuum effective theory the operator  $\tilde{O}_S$  is generated at order  $\alpha_s$ , owing to the mass of the heavy quark<sup>64</sup>

$$O_S = (\bar{b}(1 - \gamma_5)q) (\bar{b}(1 - \gamma_5)q). \quad (83)$$

Furthermore, due to explicit chiral symmetry breaking, the following operators mix with  $O_L$  in the discretised theory

$$O_R = (\bar{b}\gamma_\mu(1 + \gamma_5)q) (\bar{b}\gamma_\mu(1 + \gamma_5)q), \quad (84)$$

$$\begin{aligned} O_N = & (\bar{b}\gamma_\mu(1 - \gamma_5)q) (\bar{b}\gamma_\mu(1 + \gamma_5)q), \\ & + (\bar{b}\gamma_\mu(1 + \gamma_5)q) (\bar{b}\gamma_\mu(1 - \gamma_5)q), \\ & + 2(\bar{b}(1 - \gamma_5)q) (\bar{b}(1 + \gamma_5)q), \\ & + 2(\bar{b}(1 + \gamma_5)q) (\bar{b}(1 - \gamma_5)q). \end{aligned} \quad (85)$$

The relation between the  $B$  parameter in the full theory and the relevant operator matrix elements in the effective lattice theory is then given by

$$B_B(m_b) = \frac{\sum_X Z_X^{\text{stat}} \langle \bar{B}^0 | \hat{O}_X(a) | B^0 \rangle}{\frac{8}{3} (Z_A^{\text{stat}} \langle 0 | A_4 | B^0 \rangle)^2}, \quad X = L, R, N, S \quad (86)$$

Here the matching factors  $Z_X^{\text{stat}}$  and  $Z_A^{\text{stat}}$  for the axial current are the products of the renormalisation factors required for steps 1 and 2, which are chosen such that all dependence on the scales  $\mu$  and  $a$  in  $B_B(m_b)$  vanishes. So far, only perturbative estimates exist for these matching factors, and we refer the reader to appendix A for explicit expressions. Here, we only mention that a complete matching at order  $\alpha_s$  can be performed, since the two-loop anomalous dimensions for step 1 have been computed in the  $\overline{\text{MS}}$  scheme<sup>65–68</sup>.

#### 4.2. Lattice results for $B_B$ and $B_{B_s}$

Results for the  $B$  parameter  $B_B$  are compiled in table 8. In order to facilitate the comparison of different calculations we have chosen to quote  $B_B(m_b)$  at a reference

Table 8. Results for the  $B$  parameter  $B_B(m_b)$  obtained in the quenched approximation.  $\hat{B}_B^{\text{LO}}$  and  $\hat{B}_B^{\text{NLO}}$  are the renormalisation group invariant  $B$  parameters obtained from  $B_B(m_b)$  as explained in the text. Due to our particular choice of parameters, the results for  $\hat{B}_B$  may differ slightly from those quoted in the original articles. The static approximation was used in refs. <sup>100,162,163</sup>. Furthermore, UKQCD as well as the authors of <sup>162</sup> use an improved action ( $c_{\text{sw}} = 1$ ) for the light quark sector.

Collab.	$\beta$	$B_B(\mu)$	$B_B(m_b)$	$\hat{B}_B^{\text{LO}}$	$\hat{B}_B^{\text{NLO}}$
Ken <sup>163</sup>	6.0	0.98(4)	0.97(4)	1.42(6)	1.54(6)
		$\mu = 4.33 \text{ GeV}$			
UKQCD <sup>100</sup>	6.2		0.69 $^{+3}_{-4}$ $^{+2}_{-1}$	1.02 $^{+5}_{-6}$ $^{+3}_{-2}$	1.10 $^{+5}_{-6}$ $^{+3}_{-2}$
G+M <sup>162</sup>	6.0		0.63(4)	0.92(6)	1.00(6)
			0.73(4)	1.07(6)	1.16(6)
JLQCD <sup>114</sup>	6.3		0.840(60)	1.23(9)	1.34(10)
	6.1		0.895(47)	1.31(7)	1.42(8)
B+S <sup>164</sup>	“ $\infty$ ”	0.96(6)(4)	0.89(6)(4)	1.30(9)(6)	1.42(10)(6)
		$\mu = 2 \text{ GeV}$			
ELC <sup>109</sup>	6.4	0.86(5)	0.84(5)	1.24(7)	1.34(8)
		$\mu = 3.7 \text{ GeV}$			
BDHS <sup>126</sup>	6.1	1.01(15)	0.93(14)	1.36(20)	1.48(22)
		$\mu = 2 \text{ GeV}$			

scale  $m_b = 5 \text{ GeV}$ , although some authors prefer a different value. For  $\mu < 5 \text{ GeV}$ , this conversion has been performed at leading order according to

$$B_B(m_b = 5 \text{ GeV}) = B_B(\mu) \left( \frac{\alpha_s(\mu)}{\alpha_s(m_b)} \right)^{-2/\beta_0}. \quad (87)$$

We have used the expression for  $\alpha_s(\mu)$  at leading order, viz.

$$\alpha_s^{\text{LO}}(\mu) = \frac{4\pi}{\beta_0 \ln(\mu^2/\Lambda^2)}, \quad (88)$$

which was evaluated for  $\Lambda = 200 \text{ MeV}$  and  $n_f = 4$  active quark flavours. Requiring  $\alpha_s$  to be continuous at the threshold  $\mu = m_b$ , we find  $\alpha_s^{\text{LO}}(m_b) = 0.2342$ . The value of the renormalisation group invariant  $B$  parameter  $\hat{B}_B^{\text{LO}}$  in table 8 was obtained from eq. (79) using the value of  $\alpha_s^{\text{LO}}(m_b)$ . Similarly,  $\hat{B}_B^{\text{NLO}}$  was obtained from eq. (80) by inserting the value of  $\alpha_s^{\text{NLO}}(m_b) = 0.1842$ .

By comparing the results for  $B_B(m_b)$  in the table one observes a cluster of values in the range  $0.80 - 0.90$ , as well as a few results clearly above and below, despite the fact that similar lattice spacings have been used. As was first noted in ref. <sup>100</sup>, ambiguities in the perturbative matching procedure are largely responsible for this. As the matching factors  $Z_A^{\text{stat}}$ ,  $Z_X^{\text{stat}}$ ,  $X = L, R, N, S$  in eq. (86) are themselves products of matching factors known to  $O(\alpha_s)$ , the ratios  $Z_X^{\text{stat}}/(Z_A^{\text{stat}})^2$  contain some contributions of order  $\alpha_s^2$ . By including or excluding these next-to-next-to-leading order terms, the following three possibilities can be applied:

Table 9. Results for  $B_B(m_b)$  in the static approximation for matching procedures (M<sub>1</sub>) – (M<sub>3</sub>), using results for the individual matrix elements from different groups. The couplings  $\alpha_s(\mu)$ ,  $\alpha_s(m_b)$  were evaluated using  $m_b = 5 \text{ GeV}$ ,  $n_f = 4$ ,  $\Lambda^{(4)} = 200 \text{ MeV}$ . Only statistical errors are shown. Tadpole improvement has not been applied, except that a mean field improved coupling  $\alpha_V(q^*)$  at  $aq^* = 2.18$  has been used.

method	$\alpha_s(m_b)$	UKQCD <sup>100</sup>	G+M <sup>162</sup>	Ken <sup>163</sup>
(M <sub>1</sub> )	0.2342	0.81(4)	0.82(3)	0.87(3)
	0.1842	0.80(5)	0.81(3)	0.85(3)
(M <sub>2</sub> )	0.2342	0.60(4)	0.59(3)	0.42(3)
	0.1842	0.64(5)	0.64(3)	0.51(3)
(M <sub>3</sub> )	0.2342	0.87(5)	0.83(2)	0.96(3)
	0.1842	0.88(5)	0.85(3)	0.98(3)

(M<sub>1</sub>) include  $O(\alpha_s^2)$  contributions by using the ratios  $Z_X^{\text{stat}}/(Z_A^{\text{stat}})^2$ .

(M<sub>2</sub>) exclude  $O(\alpha_s^2)$  contributions in the individual  $Z$ -factors by expanding  $Z_X^{\text{stat}}$  and  $Z_A^{\text{stat}}$  separately to order  $\alpha_s$ .

(M<sub>3</sub>) exclude  $O(\alpha_s^2)$  contributions by expanding the ratios  $Z_X^{\text{stat}}/(Z_A^{\text{stat}})^2$  to order  $\alpha_s$ .

In ref. <sup>163</sup> it was suggested that the low values for  $B_B(m_b)$  reported by UKQCD were due to using procedure (M<sub>2</sub>), and that therefore the large discrepancy between refs. <sup>163</sup> and <sup>100</sup> could largely be explained by the amplification of ambiguities by employing a particular matching procedure, rather than the different values of  $c_{\text{sw}}$  or  $\beta$  in the two simulations. In view of this issue, we wish to test the consistency of results from different groups, by listing in table 9 the values for  $B_B(m_b)$  from refs. <sup>100,162,163</sup>, which were obtained by applying methods (M<sub>1</sub>), (M<sub>2</sub>) and (M<sub>3</sub>) for uniform choices of input parameters. Indeed it turns out that method (M<sub>2</sub>) systematically produces lower values of  $B_B(m_b)$ . However, for each common procedure the discrepancy between the results for  $c_{\text{sw}} = 0$  (ref. <sup>163</sup>) and  $c_{\text{sw}} = 1$  (refs. <sup>100,162</sup>) cannot fully be resolved, so that other effects must also contribute to the observed differences.

One concludes that, although different prescriptions should be equivalent in principle, there are discrepancies of up to 25% in the final values of  $B_B(m_b)$  for  $c_{\text{sw}} = 1$  and even larger variations for unimproved Wilson fermions. As each of the methods (M<sub>1</sub>) – (M<sub>3</sub>) is perfectly justified, these differences may be viewed as a systematic error on  $B_B$  as a result of perturbative matching. As far as lattice results for  $B_B$  in the static approximation are concerned, these ambiguities do not arise exclusively from the discretisation of the theory, since the matching step between the continuum full and continuum effective theories contains a large  $O(\alpha_s)$  contribution (see also appendix A). This problem can only be addressed in a two-loop calculation for this matching step.

Different procedures should eventually yield the same answer in the continuum limit, provided that lattice artefacts are not so large as to spoil the extrapolation

$a \rightarrow 0$ . Clearly, the currently available data for  $B_B$  do not allow for such an extrapolation as in the case of decay constants discussed in the previous section. However, preliminary results in the continuum limit for  $B_B$  and some SU(3)-flavour breaking ratios involving the  $B$  parameter have been reported<sup>164,165</sup>. Also, by comparing the results from refs.<sup>100,162</sup>, which were both obtained for  $c_{\text{sw}} = 1$ , one observes only a weak dependence on the lattice spacing  $a$ .

In the absence of further data which might clarify the issues of matching as well as the influence of lattice artefacts and the size of  $1/M$  corrections to the results in the static approximation, we resort to quoting a central result for  $B_B$  with an error which encompasses the observed variations. Our best estimate is

$$B_B(m_b) = 0.85^{+13}_{-22}, \quad (89)$$

which corresponds to

$$\hat{B}_B^{\text{LO}} = 1.24^{+18}_{-32}, \quad \hat{B}_B^{\text{NLO}} = 1.35^{+21}_{-35}, \quad (90)$$

so that our final estimate for the renormalisation group invariant  $B$  parameter can be summarised as

$$\hat{B}_B = 1.3^{+2}_{-3}. \quad (91)$$

These numbers can be compared with the results from QCD sum rules. The authors of ref.<sup>166</sup> obtain  $B_B(5 \text{ GeV}) = 0.99(15)$ , which, in view of the large errors, is in agreement with our estimate. An earlier attempt to calculate the matrix element of  $O_L$  in the sum rule approach resulted in a very low value<sup>167</sup>.

We can combine our value for  $\hat{B}_B$  with the result for the decay constant  $f_B$  in the previous section. Using  $f_B = 172^{+22}_{-31} \text{ MeV}$  from table 7, we find

$$f_B \sqrt{\hat{B}_B} = 195^{+30}_{-40} \text{ MeV}. \quad (92)$$

This is one of the central results of this review and can be taken as the present estimate for this quantity treating as many individual results as possible on an equal footing.

Now we turn the discussion to SU(3)-flavour breaking ratios involving the  $B$  parameter and the decay constant. As becomes clear from table 10 the  $B$  parameter shows very little dependence on the mass of the light quark, quite in contrast to the decay constant. The results for  $B_{B_s}/B_{B_d}$  can therefore be summarised by the value

$$B_{B_s}/B_{B_d} = 1.00(2). \quad (93)$$

The result can be combined with our estimate of  $f_{B_s}/f_{B_d} = 1.14(8)$  in table 7 and eq. (75) to compute the ratio

$$\xi_{sd}^2 = \frac{f_{B_s}^2 B_{B_s}}{f_{B_d}^2 B_{B_d}} = 1.30(18). \quad (94)$$

Table 10. Results for the SU(3)-flavour breaking ratio  $B_{B_s}/B_{B_d}$  and the ratio  $\xi_{sd}^2$  defined in eq. (94). Note that  $\widehat{B}_{B_s}/\widehat{B}_{B_d} = B_{B_s}(m_b)/B_{B_d}(m_b)$ , and thus this ratio is independent of the details of the conversion to the renormalisation group invariant  $B$  parameter.

Collab.	$\beta$	$B_{B_s}/B_{B_d}$	$\xi_{sd}^2$	Comments
Ken <sup>163</sup>	6.0	$0.99^{+1}_{-1}(1)$		static, $c_{\text{sw}} = 0$
G+M <sup>162</sup>	6.0	1.01(1)	1.38(7)	static, $c_{\text{sw}} = 1$
UKQCD <sup>100</sup>	6.2	1.02(2)	$1.34^{+9}_{-8}^{+5}_{-3}$	static, $c_{\text{sw}} = 1$
JLQCD <sup>114</sup>	6.3	1.05(3)		conv., $c_{\text{sw}} = 0$
	6.1	0.99(3)		conv., $c_{\text{sw}} = 0$
BBS <sup>165</sup>	“ $\infty$ ”		1.49(13)(31)	conv., $c_{\text{sw}} = 0$
this work			1.30(18)	eqs. (75, 93)

More results for  $\xi_{sd}^2$ , which have not been used in the derivation of this result, are listed in table 10. It is worth noting that apart from the estimates for  $\xi_{sd}^2$  in the static approximation (ref.<sup>100,162</sup>), there is also a preliminary result<sup>165</sup> which treats heavy quarks in the conventional approach. Moreover, in that study  $\xi_{sd}^2$  was computed directly from the ratio of operator matrix elements, viz.

$$r_{sd} \equiv \frac{\langle \overline{B_s^0} | \widehat{O}_L | B_s^0 \rangle}{\langle \overline{B_d^0} | \widehat{O}_L | B_d^0 \rangle} = \xi_{sd}^2 \frac{M_{B_s}}{M_{B_d}} \quad (95)$$

over a range of lattice spacings. The results in table 10 and their statistical errors can be combined in a weighted average to yield

$$\xi_{sd}^2 = 1.38(15), \quad (96)$$

where we have added in quadrature a systematic error estimated from the spread of central values in the table.

## 5. Analysis of CP violation

In this section we shall combine lattice results with experimental data and other theoretical estimates to place constraints on the most poorly known elements of the CKM matrix and on the unitarity triangle.

### 5.1. Parametrisations of the CKM matrix and the unitarity triangle

We start the discussion by recalling the basic definitions and relations involving the CKM matrix. As is well known, the CKM matrix  $V_{\text{CKM}}$  relates the gauge eigenstates appearing in the SM Lagrangian to mass eigenstates. For flavour-changing charged current transitions this has the consequence that, in addition to the dominant transitions between up- and down-type quarks,  $u \leftrightarrow d$ ,  $c \leftrightarrow s$  and  $t \leftrightarrow b$ , there are further transitions of lesser strength. The corresponding Lagrangian describing

flavour-changing charged current interactions in the hadronic sector has the form

$$\mathcal{L}_{\text{CC}}^{\text{had}} = -\frac{g}{\sqrt{8}}(\bar{u}, \bar{c}, \bar{t})\gamma^\mu(1 - \gamma_5)V_{\text{CKM}}\begin{pmatrix} d \\ s \\ b \end{pmatrix}W_\mu^\dagger + \text{h.c.}, \quad (97)$$

where the CKM matrix

$$V_{\text{CKM}} = \begin{pmatrix} V_{ud} & V_{us} & V_{ub} \\ V_{cd} & V_{cs} & V_{cb} \\ V_{td} & V_{ts} & V_{tb} \end{pmatrix} \quad (98)$$

is a unitary matrix in flavour space. Since the dominant transitions are proportional to the diagonal matrix elements  $V_{ud}$ ,  $V_{cs}$  and  $V_{tb}$ , one expects a hierarchical structure of  $V_{\text{CKM}}$ . An approximate parametrisation of the CKM matrix which takes account of this structure is due to Wolfenstein<sup>168</sup>. By expanding  $V_{\text{CKM}}$  in powers of the Cabibbo angle  $|V_{us}| = \lambda \simeq 0.22$  to order  $\lambda^3$  one obtains

$$V_{\text{CKM}} \simeq \begin{pmatrix} 1 - \frac{\lambda^2}{2} & \lambda & A\lambda^3(\rho - i\eta) \\ -\lambda & 1 - \frac{\lambda^2}{2} & A\lambda^2 \\ A\lambda^3(1 - \rho - i\eta) & -A\lambda^2 & 1 \end{pmatrix}, \quad (99)$$

with the remaining parameters  $A$ ,  $\rho$  and  $\eta$  of order one.

In the case of three generations of quarks and leptons,  $V_{\text{CKM}}$  can be parametrised in terms of three angles and one observable complex phase, of which the latter is required to describe CP violation. As has been pointed out in ref.<sup>169</sup>, a consistent treatment of CP-violating effects necessitates the inclusion of higher terms in the Wolfenstein parametrisation, viz.

$$V_{\text{CKM}} \simeq \begin{pmatrix} 1 - \frac{\lambda^2}{2} & \lambda & A\lambda^3(\rho - i\eta) \\ -\lambda - iA^2\lambda^5\eta & 1 - \frac{\lambda^2}{2} & A\lambda^2 \\ A\lambda^3(1 - \bar{\rho} - i\bar{\eta}) & -A\lambda^2 - iA\lambda^4\eta & 1 \end{pmatrix}, \quad (100)$$

where the rescaled parameters  $\bar{\rho}$  and  $\bar{\eta}$  are expanded as

$$\bar{\rho} = \rho\left(1 - \frac{\lambda^2}{2} + O(\lambda^4)\right), \quad \bar{\eta} = \eta\left(1 - \frac{\lambda^2}{2} + O(\lambda^4)\right). \quad (101)$$

The relative size of CKM matrix elements is easily recognised in the Wolfenstein parametrisation: the diagonal elements are of order one, and  $|V_{us}|$ ,  $|V_{cd}|$  are both of order 20 %. The relative size of  $|V_{cb}|$  and  $|V_{ts}|$  are 4 %, whereas  $|V_{ub}|$  and  $|V_{td}|$  are of order 1 %.

The Wolfenstein parameters  $\lambda$  and  $A$  are rather well determined experimentally<sup>149,170,174,176</sup>

$$\lambda = |V_{us}| = 0.2205 \pm 0.0018 \quad (102)$$

$$A = \left| \frac{V_{cb}}{V_{us}^2} \right| = 0.81 \pm 0.058, \quad (103)$$

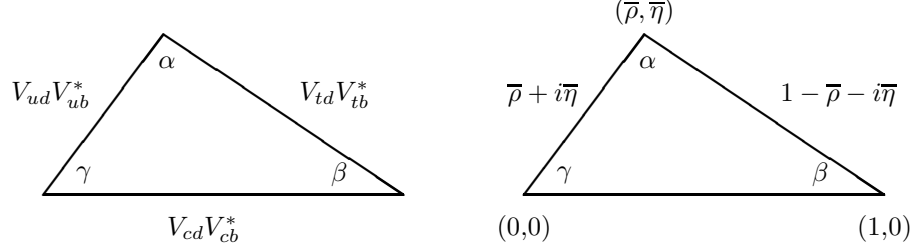


Fig. 7. The unitarity triangle corresponding to eq. (105) and its rescaled version obtained in the  $(\bar{\rho}, \bar{\eta})$ -plane by dividing all sides by  $V_{cd}V_{cb}^*$ .

whereas the elements  $|V_{ub}|$  and  $|V_{td}|$  have uncertainties of around 30 %, so that the parameters  $\rho$  and  $\eta$  are rather poorly known.

The unitarity of  $V_{\text{CKM}}$  imposes the following conditions on its elements

$$V_{ij} V_{ik}^* = 0, \quad j \neq k. \quad (104)$$

There are six such conditions, each of which can be represented graphically by a triangle. The triangle relation for the most poorly known CKM matrix elements reads

$$V_{ud}V_{ub}^* + V_{cd}V_{cb}^* + V_{td}V_{tb}^* = 0, \quad (105)$$

and its representation is shown in figure 7.

In order to constrain the values of  $\rho$  and  $\eta$  one needs information on  $|V_{td}|$ , which can be extracted from  $B^0-\bar{B}^0$  mixing. The expression for the mass difference  $\Delta M_d$  between the  $B_d^0$  and  $\bar{B}_d^0$  states reads

$$\Delta M_d = \frac{G_F^2 M_W^2}{6\pi^2} \eta_{B_d} S(m_t/M_W) f_{B_d}^2 \hat{B}_{B_d} |V_{td}V_{tb}^*|^2, \quad (106)$$

where  $G_F$  is the Fermi constant, and  $M_W$  is the mass of the  $W$ -boson. The quantity  $\eta_{B_d} = 0.55 \pm 0.01$ <sup>161</sup> parametrises QCD short-distance corrections, and  $S(m_t/M_W)$  is a slowly varying function of  $m_t/M_W$ <sup>177,178</sup>. In the following we shall evaluate the above expression using our lattice estimate for  $f_{B_d} \sqrt{\hat{B}_{B_d}}$ .

## 5.2. Constraints on the Wolfenstein parameters $\rho$ and $\eta$

Using lattice data in conjunction with experimental data and other theoretical estimates, we now want to analyse  $B_d^0-\bar{B}_d^0$  and  $B_s^0-\bar{B}_s^0$  mixing in order to place constraints on the parameters  $\rho$  and  $\eta$  discussed in the last subsection.

As is obvious from eq. (106), the quantity  $f_{B_d} \sqrt{\hat{B}_{B_d}}$  plays a central rôle in this study. Further input parameters are the running mass of the top quark,  $\bar{m}_t(m_t)$ , the short-distance corrections  $\eta_{B_d}$  and the experimentally measured value of  $\Delta M_d$ . For  $B_s^0-\bar{B}_s^0$  mixing, the quantity  $\xi_{sd}^2$  is also required. A compilation of input parameters for this study is listed in table 11.

Solving for  $|V_{td}|$  in eq. (106) and inserting the relevant input parameters as well as  $\eta_B = 0.55 \pm 0.01$ , one finds

$$|V_{td}| = (8.94^{+1.43}_{-1.88}) \times 10^{-3}, \quad (107)$$

and thus the relative uncertainty in  $|V_{td}|$  according to this estimate amounts to 15 – 20 %. The results for  $|V_{td}|$  can be translated into a constraint on  $\bar{\rho}$  and  $\bar{\eta}$  via the unitarity triangle

$$\sqrt{(1 - \bar{\rho})^2 + \bar{\eta}^2} = \frac{1}{\lambda} \left| \frac{V_{td}}{V_{cb}} \right| = 1.03^{+0.18}_{-0.23}, \quad (108)$$

where we have used the present determination of  $|V_{cb}|^{170,174}$

$$|V_{cb}| = 0.0393 \pm 0.0028. \quad (109)$$

Further constraints on  $\rho$  and  $\eta$  can be obtained from indirect CP violation in the  $K^0 - \bar{K}^0$  system through a theoretical analysis of the parameter  $\epsilon_K^{179,180,181}$ . This requires as additional input an estimate for the kaon  $B$  parameter  $\hat{B}_K$ . Several theoretical methods, including lattice simulations,<sup>164,182–189</sup> quote values for  $\hat{B}_K$  which are compatible with the range

$$\hat{B}_K = 0.75 \pm 0.10. \quad (110)$$

There has been considerable progress in calculating  $\hat{B}_K$  on the lattice<sup>189</sup>. However, a number of systematic effects such as the continuum limit, the chiral behaviour of  $\hat{B}_K$  computed using Wilson fermions, and the dependence on the number of flavour require further studies<sup>190–193</sup>. A more detailed discussion of lattice results for  $\hat{B}_K$  is, however, beyond the scope of this review.

Herrlich and Nierste<sup>180</sup> have obtained constraints on  $\bar{\rho}$  and  $\bar{\eta}$  from a theoretical analysis of  $\epsilon_K$  using the complete  $\Delta S = 2$  effective hamiltonian at next-to-leading order. Using very similar estimates for  $f_{B_d} \sqrt{\hat{B}_{B_d}}$  and  $\xi_{sd}^2$  (i.e.  $f_{B_d} \sqrt{\hat{B}_{B_d}} = 200 \pm 40$  MeV,  $\xi_{sd}^2 = 1.32 \pm 0.12$ ) compared to this review, they find

$$-0.20 \leq \bar{\rho} \leq 0.22, \quad 0.25 \leq \bar{\eta} \leq 0.43, \quad (111)$$

Table 11. Input parameters for the study of  $\rho$  and  $\eta$ .

Quantity	Value	Source
$f_{B_d} \sqrt{\hat{B}_{B_d}}$	$195^{+30}_{-40}$ MeV	Lattice, this work
$\xi_{sd}^2$	$1.38 \pm 0.15$	Lattice, this work
$M_{B_d}$	5279 MeV	Exp. <sup>149</sup>
$M_{B_s}$	5369 MeV	Exp. <sup>149</sup>
$\Delta M_d$	$0.464 \pm 0.018$ ps <sup>-1</sup>	Exp. <sup>170</sup>
$\bar{m}_t(m_t)$	$165 \pm 9$ GeV	Exp. <sup>171,176</sup>



in good agreement with a similar study by Ali and London<sup>175,176</sup>.

Now we turn our attention to  $B_s^0-\overline{B}_s^0$  mixing. The ratio of mass differences for the  $B_d^0-\overline{B}_d^0$  and  $B_s^0-\overline{B}_s^0$  systems is

$$\frac{\Delta M_s}{\Delta M_d} = \frac{\eta_{B_s} f_{B_s}^2 \widehat{B}_{B_s}}{\eta_{B_d} f_{B_d}^2 \widehat{B}_{B_d}} \frac{M_{B_s}}{M_{B_d}} \frac{|V_{ts}|^2}{|V_{td}|^2}. \quad (112)$$

Since  $\eta_{B_s} = \eta_{B_d}$ <sup>194</sup> this becomes

$$\begin{aligned} \frac{\Delta M_s}{\Delta M_d} &= \xi_{sd}^2 \frac{M_{B_s}}{M_{B_d}} \frac{|V_{ts}|^2}{|V_{td}|^2} \\ &= (1.40 \pm 0.15) \frac{|V_{ts}|^2}{|V_{td}|^2}, \end{aligned} \quad (113)$$

where we have used the parameters listed in table 11. This result can be used together with the measured value of  $\Delta M_d$  to predict  $\Delta M_s$ , provided that the allowed range of  $|V_{ts}|^2/|V_{td}|^2$  is determined. This has been performed by Ali and London<sup>176</sup>, who have analysed  $|V_{td}|/|V_{ts}|$  as a function of  $f_{B_d} \sqrt{\widehat{B}_{B_d}}$ , assuming that  $\widehat{B}_K = 0.75 \pm 0.10$ . Using our estimate of  $f_{B_d} \sqrt{\widehat{B}_{B_d}} = 195^{+30}_{-40}$  MeV one reads off the allowed range of  $|V_{td}|/|V_{ts}|$  from figure 4 in ref.<sup>176</sup>

$$\frac{|V_{td}|}{|V_{ts}|} = 0.228 \pm 0.040^{+0.050}_{-0.035}, \quad (114)$$

where the first error is due to the uncertainty in  $\widehat{B}_K$ , and the second reflects the error on  $f_{B_d} \sqrt{\widehat{B}_{B_d}}$ . This yields

$$\Delta M_s = 12.5 \pm 0.48 \pm 1.3 \pm 4.4^{+5.5}_{-3.8} \text{ ps}^{-1}. \quad (115)$$

Here the first error is due to the experimental error on  $\Delta M_d$ , the second due to the error in  $\xi_{sd}^2$ , and the third and fourth to the uncertainties in the matrix elements  $\widehat{B}_K$  and  $f_{B_d} \sqrt{\widehat{B}_{B_d}}$ , respectively. Adding the errors in quadrature one gets

$$\Delta M_s = 12.5^{+7.2}_{-6.0} \text{ ps}^{-1}. \quad (116)$$

Using the updated results for the  $B_s$  lifetime,  $\tau_{B_s} = 1.61 \pm 0.10 \text{ ps}$ <sup>149</sup>, this corresponds to a value for the  $B_s^0-\overline{B}_s^0$  mixing parameter  $x_s$  of

$$x_s = 20.1^{+11.6}_{-9.7}. \quad (117)$$

Our estimates for  $\Delta M_s$  and  $x_s$  can be compared to the experimental lower bound of

$$\Delta M_s > 7.8 \text{ ps}^{-1}, \quad x_s > 12.6 \quad (95\% \text{ C.L.}) \quad (118)$$

quoted by the ALEPH Collaboration<sup>170,172,173</sup>. This indicates that, although the experimental lower bound is still smaller than the central value of the SM prediction,

experiments start to exclude parts of the allowed range of  $\Delta M_s$ . Therefore, experimental data for  $\Delta M_d$  and  $\Delta M_s$  can further restrict the allowed range of  $(\overline{\rho}, \overline{\eta})$ , a fact that has already been exploited in deriving the constraints in eq. (111)<sup>181</sup>.

The constraints on CKM parameters have sharpened significantly in recent years, not least thanks to more accurate and consistent determinations of weak matrix elements using lattice techniques.

## 6. Concluding Remarks

In this review we have combined a variety of lattice results for heavy-light decay constants and the  $B$  parameter  $B_B$  into a common estimate for  $f_B\sqrt{B_B}$ . A central part of this study was the analysis of the continuum limit of decay constants and the assessment of systematic errors. Our result for  $f_B\sqrt{B_B}$  has been combined with other theoretical and experimental input to constrain some of the CKM matrix elements. Although the overall errors on lattice results in the heavy quark sector are still rather large, the progress in lattice calculations over the past years has helped a lot in order to sharpen the bounds on CKM matrix elements and the unitarity triangle.

The interplay between different theoretical tools plays an important rôle in this analysis, as it serves to extract a consistent picture in situations where each method has its own limitations. An example for this is the study of  $1/M$  corrections to the scaling law for decay constants. Lattice simulations are currently limited by a number of systematic effects, such as quenching, which cannot fully be addressed at present due to lack of resources. However, in order to increase the precision of lattice calculations, not only larger computing power but also new theoretical ideas such as non-perturbative improvement, are of great importance.

Here we have concentrated on leptonic decays of heavy quarks. This is by no means the only area where lattice calculations have made an impact on the determination of CKM matrix elements. Indeed, another poorly known element,  $V_{ub}$ , can be determined by considering semi-leptonic  $B$  decays, such as  $B \rightarrow \pi \ell \nu_\ell$  or  $B \rightarrow \rho \ell \nu_\ell$ . Lattice simulations offer model-independent estimates for the relevant form factors, and a variety of calculations has already been performed<sup>18</sup>. Likewise, lattice results for rare decays such as  $B \rightarrow K^* \gamma$  have been reported in the past few years. All of these calculations serve ultimately to test the consistency of the Standard Model, and it is evident that the lattice is a versatile tool in these analyses.

With the advent of dedicated experimental facilities for  $B$  physics, such as HERA-B, BaBar and LHC-B, together with an improved theoretical understanding of heavy quark physics, the scene is set for an exciting new period in particle physics.

## Acknowledgements

I would like to thank my colleagues in the UKQCD Collaboration, and in particular Chris Sachrajda for the fruitful collaboration on some of the topics reviewed

in this work. Furthermore, I would like to thank Dina Alexandrou, Chris Allton, Claude Bernard, Jonathan Flynn, Shoji Hashimoto, Fred Jegerlehner, Rainer Sommer and Mike Teper for interesting discussions. Special thanks go to Chris Allton, Claude Bernard and Shoji Hashimoto for communicating some of their results prior to publication, and to Vicente Giménez for useful exchanges about matching factors for the  $B$  parameter. The support of the Particle Physics and Astronomy Research Council (PPARC) through the award of an Advanced Fellowship is gratefully acknowledged.

## Appendix A. Matching Factors for the Static Approximation

In this appendix we list the expressions for the perturbative matching factors for the heavy-light axial current and the  $\Delta B = 2$  four-fermion operator in the static approximation. As described in subsection 4.1, the matching is usually performed in a two-step process, where one first matches the full theory in the continuum to the effective continuum theory, which is then matched to the effective theory on the lattice.

Throughout this appendix we use the following convention for the one- and two-loop coefficients of the perturbative  $\beta$  function

$$\beta_0 = 11 - \frac{2}{3}n_f, \quad \beta_1 = 102 - \frac{38}{3}n_f, \quad (\text{A.1})$$

where  $n_f$  is the number of active quark flavours.

### Appendix A.1. The axial current

A full  $O(\alpha_s)$  matching between the axial current  $A_\mu$  in full QCD and its counterpart  $\tilde{A}_\mu$  in the continuum effective theory can be performed, since the two-loop anomalous dimension of  $\tilde{A}_\mu$  has been computed<sup>65</sup>. For typical hadronic scales  $\mu < m_b$ , and using the naïve dimensional regularisation scheme one obtains<sup>60,65</sup>

$$A_\mu = \left( \frac{\alpha_s(m_b)}{\alpha_s(\mu)} \right)^{d_{1,A}} \left\{ 1 + \frac{\alpha_s(\mu) - \alpha_s(m_b)}{4\pi} J_A + \frac{\alpha_s(m_b)}{4\pi} C_2 \right\} \tilde{A}_\mu, \quad (\text{A.2})$$

where

$$C_2 = -8/3 \quad (\text{A.3})$$

and

$$d_{1,A} = \frac{\gamma_A^{(0)}}{2\beta_0}, \quad J_A = \frac{\gamma_A^{(0)}}{2\beta_0} \left( \frac{\beta_1}{\beta_0} - \frac{\gamma_A^{(1)}}{\gamma_A^{(0)}} \right), \quad (\text{A.4})$$

$$\gamma_A^{(0)} = -4, \quad \gamma_A^{(1)} = -\frac{254}{9} - \frac{56}{27}\pi^2 + \frac{20}{9}n_f. \quad (\text{A.5})$$

The general expression for the matching of the current  $\tilde{A}_\mu$  to the current  $\hat{A}_\mu$  in the effective theory on the lattice is

$$\tilde{A}_\mu = \left( 1 + \frac{\alpha_s^{\text{latt}}(\mu)}{4\pi} [2 \ln(\mu^2 a^2) + D_A] \right) \hat{A}_\mu. \quad (\text{A.6})$$

Numerical values of  $D_A$  depend on the choice of  $c_{\text{sw}}$  and are tabulated in table A.1.

Eq. (A.6) is usually evaluated using a tadpole improved or boosted value for the lattice coupling  $\alpha_s^{\text{latt}}$ , for instance  $\tilde{\alpha}_s = \alpha_s^{\text{latt}}/u_0^4$ , where  $u_0$  is the average link,  $u_0 = \langle \frac{1}{3} \text{Re Tr } P \rangle^{1/4}$ , or alternatively  $u_0 = 1/(8\kappa_{\text{crit}})$ . Combining measured values for  $u_0$  with its perturbation expansion, viz.

$$u_0 = 1 + u_0^{(1)}\alpha_s + O(\alpha_s^2) \quad (\text{A.7})$$

one can write down the tadpole improved version of eq. (A.6)

$$\tilde{A}_\mu = \sqrt{u_0} \left( 1 + \frac{\tilde{\alpha}_s(\mu)}{4\pi} [2 \ln(\mu^2 a^2) + D_A - \frac{1}{2} u_0^{(1)}] \right) \hat{A}_\mu. \quad (\text{A.8})$$

The square root of  $u_0$  has to be taken since the static-light axial current contains only one relativistic quark field. The matching factor between  $\tilde{A}_\mu$  and  $\hat{A}_\mu$  could in principle also be determined non-perturbatively using the method in ref. <sup>82</sup>. Combining the factors for the two matching steps one finds

$$\begin{aligned} Z_A^{\text{stat}} &= \left( \frac{\alpha_s(m_b)}{\alpha_s(\mu)} \right)^{d_{1,A}} \left\{ 1 + \frac{\alpha_s(\mu) - \alpha_s(m_b)}{4\pi} J_A - \frac{8}{3} \frac{\alpha_s(m_b)}{4\pi} \right\} \\ &\times \sqrt{u_0} \left( 1 + \frac{\tilde{\alpha}_s(\mu)}{4\pi} [2 \ln(\mu^2 a^2) + D_A - \frac{1}{2} u_0^{(1)}] \right). \end{aligned} \quad (\text{A.9})$$

## Appendix A.2. *The four-fermion operator*

The perturbative matching for the four-fermion operator is more complicated due to operator mixing. Apart from the operator  $O_L$ , the basis of local operators in the continuum effective theory consists also of the operator  $O_S$  defined in eq. (83). The full  $O(\alpha_s)$  matching relation between  $O_L$  and the operators  $\tilde{O}_L$  and  $\tilde{O}_S$  in the continuum effective theory is given by

$$\begin{aligned} O_L(m_b) &= \left( \frac{\alpha_s(m_b)}{\alpha_s(\mu)} \right)^{d_1} \left\{ 1 + \frac{\alpha_s(\mu) - \alpha_s(m_b)}{4\pi} J + \frac{\alpha_s(m_b)}{4\pi} B_1 \right\} \tilde{O}_L(\mu) \\ &+ \left\{ \left( \frac{\alpha_s(m_b)}{\alpha_s(\mu)} \right)^{d_2} - \left( \frac{\alpha_s(m_b)}{\alpha_s(\mu)} \right)^{d_1} \right\} \frac{\gamma_{21}^{(0)}}{\gamma_{22}^{(0)} - \gamma_{11}^{(0)}} \frac{\alpha_s(m_b)}{4\pi} B_2 \tilde{O}_L(\mu) \\ &+ \left( \frac{\alpha_s(m_b)}{\alpha_s(\mu)} \right)^{d_2} \frac{\alpha_s(m_b)}{4\pi} B_2 \tilde{O}_S(\mu), \end{aligned} \quad (\text{A.10})$$

where in naïve dimensional regularisation <sup>64</sup>

$$B_1 = -14, \quad B_2 = -8 \quad (\text{A.11})$$

and <sup>64,66–68</sup>

$$d_i = \frac{\gamma_{ii}^{(0)}}{2\beta_0}, \quad J = \frac{\gamma_{11}^{(0)}}{2\beta_0} \left( \frac{\beta_1}{\beta_0} - \frac{\gamma_{11}^{(1)}}{\gamma_{11}^{(0)}} \right), \quad (\text{A.12})$$

Table A.1. Values for the coefficients  $D_A$ ,  $D_L$ ,  $D_R$  and  $D_N$  for unimproved and improved Wilson fermions according to refs.<sup>62,64,77</sup>. In the case of the four-fermion operator for  $c_{\text{sw}} = 1$ , the conventions of ref.<sup>77</sup> are used.

$c_{\text{sw}}$	$D_A$	$D_L$	$D_R$	$D_N$
0	-27.17	-38.91	-1.61	-14.40
1	-20.20	-22.50	-5.40	-14.00

$$\gamma^{(0)} \equiv \begin{pmatrix} \gamma_{11}^{(0)} & \gamma_{12}^{(0)} \\ \gamma_{21}^{(0)} & \gamma_{22}^{(0)} \end{pmatrix} = \begin{pmatrix} -8 & 0 \\ 4/3 & -8/3 \end{pmatrix}, \quad (\text{A.13})$$

$$\gamma_{11}^{(1)} = -\frac{808}{9} - \frac{52}{27}\pi^2 + \frac{64}{9}n_f. \quad (\text{A.14})$$

When matching  $\tilde{O}_L(\mu)$  to its lattice counterpart  $\hat{O}_L(\mu)$ , one has to consider the lattice operators  $\hat{O}_R(\mu)$  and  $\hat{O}_N(\mu)$  (eqs. (84,85)), such that

$$\begin{aligned} \tilde{O}_L(\mu) &= \left(1 + \frac{\alpha_s^{\text{latt}}(\mu)}{4\pi} [4\ln(\mu^2 a^2) + D_L]\right) \hat{O}_L(a) \\ &\quad + \frac{\alpha_s^{\text{latt}}(\mu)}{4\pi} D_R \hat{O}_R(a) + \frac{\alpha_s^{\text{latt}}(\mu)}{4\pi} D_N \hat{O}_N(a). \end{aligned} \quad (\text{A.15})$$

Since  $\tilde{O}_S$  is generated at order  $\alpha_s$  one finds

$$\tilde{O}_S(\mu) = \hat{O}_S(a) + \text{higher orders}. \quad (\text{A.16})$$

Values for the coefficients  $D_L$ ,  $D_R$  and  $D_N$  have been determined for  $c_{\text{sw}} = 0$  and 1<sup>64,62,77</sup> and are listed in table A.1. We have chosen the convention that the static-light meson propagator is proportional to  $e^{-\mathcal{E}t}$ , such that the reduced value of the quark self-energy has been used<sup>61</sup> in the evaluation of  $D_A$  and  $D_L$ .

Combining the two matching steps and using tadpole improvement, we find the following expressions for the renormalisation factors  $Z_X^{\text{stat}}$ ,  $X = L, R, N, S$

$$\begin{aligned} Z_L^{\text{stat}} &= \left(\frac{\alpha_s(m_b)}{\alpha_s(\mu)}\right)^{d_1} \left\{ 1 + \frac{\alpha_s(\mu) - \alpha_s(m_b)}{4\pi} J - 14 \frac{\alpha_s(m_b)}{4\pi} \right\} \\ &\quad \times u_0 \left( 1 + \frac{\tilde{\alpha}_s(\mu)}{4\pi} [4\ln(\mu^2 a^2) + D_L - u_0^{(1)}] \right) \\ &\quad + \left\{ \left(\frac{\alpha_s(m_b)}{\alpha_s(\mu)}\right)^{d_2} - \left(\frac{\alpha_s(m_b)}{\alpha_s(\mu)}\right)^{d_1} \right\} (-2) \frac{\alpha_s(m_b)}{4\pi} \end{aligned} \quad (\text{A.17})$$

$$\begin{aligned} Z_R^{\text{stat}} &= \left(\frac{\alpha_s(m_b)}{\alpha_s(\mu)}\right)^{d_1} \left\{ 1 + \frac{\alpha_s(\mu) - \alpha_s(m_b)}{4\pi} J - 14 \frac{\alpha_s(m_b)}{4\pi} \right\} \\ &\quad \times \frac{\tilde{\alpha}_s(\mu)}{4\pi} [4\ln(\mu^2 a^2) + D_R] \end{aligned} \quad (\text{A.18})$$

$$Z_N^{\text{stat}} = \left(\frac{\alpha_s(m_b)}{\alpha_s(\mu)}\right)^{d_1} \left\{ 1 + \frac{\alpha_s(\mu) - \alpha_s(m_b)}{4\pi} J - 14 \frac{\alpha_s(m_b)}{4\pi} \right\}$$

$$\times \frac{\tilde{\alpha}_s(\mu)}{4\pi} [4 \ln(\mu^2 a^2) + D_N] \quad (\text{A.19})$$

$$Z_S^{\text{stat}} = \left( \frac{\alpha_s(m_b)}{\alpha_s(\mu)} \right)^{d_2} (-8) \frac{\alpha_s(m_b)}{4\pi}. \quad (\text{A.20})$$

One can now use the above expressions directly in the calculation of  $B_B(m_b)$  or, alternatively, perform a systematic expansion of  $Z_A^{\text{stat}}$  and  $Z_X^{\text{stat}}$ ,  $X = L, R, N, S$  to order  $\alpha_s$ . Since the  $B$  parameter is a ratio of matrix elements, another possibility is an expansion of the ratios  $Z_X^{\text{stat}}/(Z_A^{\text{stat}})^2$ ,  $X = L, R, N, S$  to order  $\alpha_s$ .

## Appendix B. Continuum Limit in the Light Quark Sector

Here we describe the continuum extrapolation of quantities in the light quark sector, which are commonly used to set the scale in lattice gauge theories. We will focus on the rho meson mass  $M_\rho$ , the pion decay constant  $f_\pi$  and the 1P–1S splitting in charmonium,  $\Delta_{1\text{P}-1\text{S}}$ .

For these three quantities the question arises whether or not they can be computed with high enough precision and reliably be extrapolated to the continuum limit:

- precise lattice estimates for  $f_\pi$  require knowledge of the current normalisation constant  $Z_A$ , which for most of the available lattice data is only known in perturbation theory.
- $M_\rho$  is usually obtained with small errors, but studies with high statistics<sup>204</sup> show oscillations in the relevant correlation functions, which, despite the fact that they can be modelled, makes it more difficult to extract a precise mass value. Furthermore, as has been discussed in ref.<sup>23</sup>, the  $a$  dependence of  $M_\rho$  computed with unimproved Wilson fermions is very strong, such that the continuum extrapolation may not be too reliable.
- the splitting  $\Delta_{1\text{P}-1\text{S}}$  shows only a weak  $a$  dependence. However, the estimates published so far have still relatively large statistical errors<sup>203</sup>.

This discussion underlines the importance of obtaining low energy quantities with higher precision, and this may now be possible using the recently proposed non-perturbatively improved Wilson action<sup>52</sup>, which is expected to yield lattice data that are completely free of lattice artefacts at order  $a$ . Since also the current normalisation constants have been determined non-perturbatively<sup>53</sup>, one can expect highly accurate continuum results for  $f_\pi$  as well. For the time being, however, we must restrict our attention to the unimproved Wilson case, as lattice data for improved actions are not yet available over a large enough range in  $\beta$  to allow for a continuum extrapolation.

The extrapolation of hadronic quantities in the light quark sector proceeds by forming dimensionless ratios, say  $f_\pi/\sqrt{\sigma}$ , using lattice data for the string tension, and extrapolating it to the continuum limit as a function of  $a\sqrt{\sigma}$ . In table B.1

Table B.1. Lattice results for the string tension  $a\sqrt{\sigma}$ .

$\beta$	$a\sqrt{\sigma}$	Author
6.8	0.0730(12)	Bali & Schilling <sup>196</sup>
6.5	0.1068(10)	UKQCD <sup>195</sup>
6.4	0.1215(12)	Bali & Schilling <sup>196</sup>
	0.1218(5)(23)	UKQCD <sup>198</sup>
	0.1216(11)	combined
6.2	0.1619(19)	Bali & Schilling <sup>196</sup>
	0.1609(28)	UKQCD <sup>199</sup>
	0.1608(7)(16)	UKQCD <sup>198</sup>
	0.1612(12)	combined
6.0	0.2265(55)	Bali & Schilling <sup>196</sup>
	0.2182(21)	Michael & Perantonis <sup>200</sup>
	0.2154(10)(40)	UKQCD <sup>198</sup>
	0.2185(18)	combined
5.9	0.2702(37)	MTc <sup>201</sup>
5.8	0.3302(30)	MTc <sup>201</sup>
5.7	0.4099(24)	MTc <sup>201</sup>

we list the lattice data for the string tension that have been used throughout this review. In cases when several estimates are available at one  $\beta$  value they have been combined in a weighted average. Estimates of  $a\sqrt{\sigma}$  at “intermediate” values of  $\beta$  (e.g.  $\beta = 6.17$ ) were then obtained by linear interpolation of  $\ln(a\sqrt{\sigma})$  as a function of  $\beta$ .

The conceptual advantages of the hadronic scale  $r_0$  described in ref.<sup>45</sup> make it an ideal quantity to perform the extrapolation to the continuum limit. A compilation of lattice results for  $r_0/a$  can be found in table B.2. Since  $r_0/a$  is so far only available for  $\beta \geq 6.0$ , the Wilson data at lower  $\beta$  values (in both the light and heavy quark sectors) cannot be used in the extrapolations to  $a = 0$ . Thus, we have decided

Table B.2. Lattice results for the hadronic scale  $r_0/a$ .

$\beta$	$r_0/a$	Author
6.5	11.23(21)	UKQCD <sup>195,197</sup>
6.4	9.90(54)	Bali & Schilling <sup>196,197</sup>
	9.75(17)	UKQCD <sup>198</sup>
6.2	7.38(25)	Bali & Schilling <sup>196,197</sup>
	7.29(17)	UKQCD <sup>198</sup>
	7.27(3)	SESAM <sup>202</sup>
6.0	5.44(26)	Bali & Schilling <sup>196,197</sup>
	5.47(11)	UKQCD <sup>198</sup>
	5.35 <sup>+2</sup> <sub>-3</sub>	SESAM <sup>202</sup>

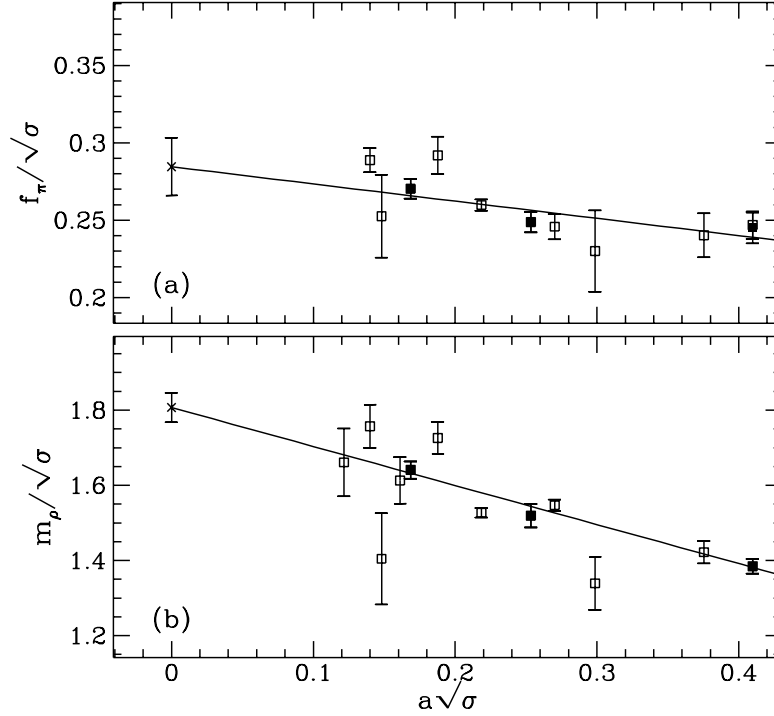


Fig. B.1. Extrapolation of: (a)  $f_\pi/\sqrt{\sigma}$  from ref. <sup>205</sup>, (b)  $M_\rho/\sqrt{\sigma}$  from ref. <sup>206</sup> to the continuum limit (full squares). Open squares denote the data for  $f_\pi$  from refs. <sup>99,102,116,128,133,207,209,211</sup> and for  $M_\rho$  from refs. <sup>98,128,133,207–211</sup>. Data at the same value of  $\beta$  have been combined.

to use the string tension, keeping in mind that eventually  $r_0$  should be used when more precision results for hadronic quantities become available.

In order to obtain  $f_\pi/\sqrt{\sigma}$  and  $M_\rho/\sqrt{\sigma}$  in the continuum limit, we shall use the results quoted by the GF11 collaboration<sup>205,206</sup>. Their simulations were intended as a comprehensive study of the continuum and infinite volume limits of the light hadronic sector in the unimproved Wilson theory. There are, in fact, many more lattice results for  $f_\pi$  and  $M_\rho$ <sup>98,99,102,109,116,128,133,207–211</sup>, also for improved actions<sup>133,210–214</sup>, and mostly with small statistical errors. However, a reliable continuum extrapolation of all available data is difficult to perform without a consistent treatment of systematic errors. This is the main reason why we have chosen to use only GF11's results in the present study. The accuracy and reliability of the extrapolated values can be checked by comparing to other simulations.

In figure B.1 (a) we show the continuum extrapolation of  $f_\pi/\sqrt{\sigma}$ . For the axial current normalisation factor  $Z_A$  we used the tadpole improved perturbative expression evaluated using the boosted coupling  $g_P^2 = g_0^2/u_0^4$ . It is seen that most other simulations are in fact consistent with GF11's data. In principle the error on the extrapolated result could be reduced by including more data points. However, this would imply a very selective use of the available data, since overall compatibility of



all results is hard to achieve.

At zero lattice spacing we obtain

$$\left. \frac{f_\pi}{\sqrt{\sigma}} \right|_{a=0} = 0.285(13). \quad (\text{B.1})$$

We have checked the stability of this result by using different prescriptions to evaluate  $Z_A$  and find that the resulting variation is much smaller than the quoted error.

Figure B.1 (b) shows the corresponding extrapolation of  $M_\rho/\sqrt{\sigma}$ . The result at  $a = 0$  is

$$\left. \frac{M_\rho}{\sqrt{\sigma}} \right|_{a=0} = 1.807(39). \quad (\text{B.2})$$

The figure illustrates the strong  $a$  dependence of this ratio in the unimproved Wilson theory (note that  $M_\rho/\sqrt{\sigma}$  is plotted on a much smaller scale than  $f_\pi/\sqrt{\sigma}$ ). It is, however, reassuring to notice that more recent simulations using a non-perturbative value of  $c_{\text{sw}}$ <sup>210,215</sup> obtain values for  $M_\rho/\sqrt{\sigma}$  which are consistent with the extrapolated Wilson result, whilst showing very little residual  $a$  dependence.

In order to compute  $\Delta_{1\text{P}-1\text{S}}/\sqrt{\sigma}$  in the continuum limit we have extrapolated the results quoted in ref.<sup>203</sup> and obtain

$$\left. \frac{\Delta_{1\text{P}-1\text{S}}}{\sqrt{\sigma}} \right|_{a=0} = 1.01(12). \quad (\text{B.3})$$

It should be emphasised that the non-perturbatively improved action<sup>52</sup> could be used to obtain much more precise estimates of the above quantities. One will thus be able to set the scale much more reliably in future simulations.

## References

1. M.A. Shifman, A.I. Vainshtein, V.I. Zakharov, *Nucl. Phys. B* **147**, 385 (1979); L.J. Reinders, H.R. Rubinstein, S. Yazaki, *Phys. Rep.* **127**, 1 (1985).
2. K.G. Wilson, *Phys. Rev. D* **10**, 2445 (1974).
3. K.G. Wilson, in: *New Phenomena in Subnuclear Physics*, ed. A. Zichichi (Plenum Press, New York 1975), p. 69.
4. E. Shuryak, *Nucl. Phys. B* **198**, 83 (1982).
5. M.B. Voloshin and M.A. Shifman, *Sov. J. Nucl. Phys.* **45**, 292 (1987); *Sov. J. Nucl. Phys.* **47**, 511 (1988).
6. N. Isgur and M.B. Wise, *Phys. Lett. B* **232**, 113 (1989); *Phys. Lett. B* **237**, 527 (1990).
7. E. Eichten and F. Feinberg, *Phys. Rev. Lett.* **43**, 1205 (1979); *Phys. Rev. D* **23**, 2724 (1981).
8. W.E. Caswell and G.P. Lepage, *Phys. Lett. B* **167**, 437 (1986).
9. E. Eichten, *Nucl. Phys. B (Proc. Suppl.)* **4**, 170 (1988).
10. H.D. Politzer and M. Wise, *Phys. Lett. B* **206**, 681 (1988); *Phys. Lett. B* **208**, 504 (1988).
11. H. Georgi, *Phys. Lett. B* **240**, 447 (1990).
12. For reviews on this subject see: M. Neubert, *Phys. Rep.* **245**, 259 (1994); M. Shifman, in: *QCD and Beyond*, proceedings of Theoretical Advanced Study Institute in Elementary Particle Physics (TASI 95), Boulder, CO, 1995, [hep-ph/9510377](#); M. Neubert, *Int. J. Mod. Phys. A* **11**, 4173 (1996).

13. K. Wilson, *Phys. Rev.* **179**, 1499 (1969).
14. C.T. Sachrajda, *Nucl. Phys. B (Proc. Suppl.)* **30**, 20 (1993).
15. C.W. Bernard, *Nucl. Phys. B (Proc. Suppl.)* **34**, 47 (1994).
16. R. Sommer, *Nucl. Phys. B (Proc. Suppl.)* **42**, 186 (1995).
17. C. Allton, *Nucl. Phys. B (Proc. Suppl.)* **47**, 31 (1996).
18. J.M. Flynn, *Nucl. Phys. B (Proc. Suppl.)* **53**, 168 (1997).
19. C. Bernard, *Weak Matrix Elements on and off the Lattice*, Lectures given at TASI '89, Boulder, CO, 4–30 June, 1989, NSF-ITP-89-152.
20. C.W. Bernard and A. Soni, *Lattice Approach to Electroweak Matrix Elements*, BNL-47585, 1992.
21. C.T. Sachrajda, *B Physics from Lattice QCD*, in: *B Decays*, revised 2<sup>nd</sup> edition, S. Stone (ed.) (World Scientific, Singapore, 1994), p. 602.
22. A.S. Kronfeld and P.B. Mackenzie, *Ann. Rev. Nucl. Part. Sci.* **43**, 793 (1993).
23. R. Sommer, *Phys. Rep.* **275**, 47 (1996).
24. H. Wittig, proceedings of the 3rd German-Russian Workshop on Progress in Heavy Quark Physics, Dubna, Russia, 20–22 May 1996, p. 7, [hep-ph/9606371](#).
25. G. Martinelli, *Nucl. Instrum. Meth. A* **384**, 241 (1996).
26. J.M. Flynn, presented at 28th International Conference on High-Energy Physics (ICHEP 96), Warsaw, Poland, 25–31 Jul 1996, [hep-lat/9611016](#).
27. M. Creutz, *Quarks, Gluons And Lattices* (Cambridge University Press, Cambridge, 1983).
28. H.J. Rothe, *Lattice Gauge Theories: An Introduction* (World Scientific, Singapore, 1992).
29. I. Montvay and G. Münster *Quantum Fields on a Lattice* (Cambridge University Press, Cambridge, 1994).
30. J. Kogut and L. Susskind, *Phys. Rev. D* **11**, 395 (1975); T. Banks, J. Kogut and L. Susskind, *Phys. Rev. D* **13**, 1043 (1976); L. Susskind, *Phys. Rev. D* **16**, 3031 (1976).
31. H.S. Sharatchandra, H.J. Thun and P. Weisz, *Nucl. Phys. B* **192**, 205 (1981); M.F.L. Golterman and J. Smit, *Nucl. Phys. B* **245**, 61 (1984); S. Sharpe, *Nucl. Phys. B (Proc. Suppl.)* **26**, 197 (1992).
32. S. Duane, A.D. Kennedy, B.J. Pendleton and D. Roweth, *Phys. Lett. B* **195**, 216 (1987).
33. A.M. Horowitz, *Nucl. Phys. B* **280**, 510 (1987), *Phys. Lett. B* **268**, 247 (1991).
34. M. Lüscher, *Nucl. Phys. B* **418**, 637 (1994).
35. H. Hamber and G. Parisi, *Phys. Rev. Lett.* **47**, 1792 (1981); E. Marinari, G. Parisi and C. Rebbi, *Phys. Rev. Lett.* **47**, 1795 (1981).
36. D. Weingarten, *Phys. Lett. B* **109**, 57 (1982).
37. A.V. Aho, J.E. Hopcroft and J.D. Ullmann, *The Design and Analysis of Computer Algorithms* (Addison Wesley, Reading, 1974); J. Stoer and R. Bulirsch, *Introduction to Numerical Analysis* (Springer, Berlin, 1980); P. Rossi, C.T.H. Davies and G.P. Lepage, *Nucl. Phys. B* **297**, 287 (1988).
38. H. van der Vorst, *SIAM J. Sc. Stat. Comp.* **13**, 631 (1992); A. Frommer *et al.*, *Int. J. Mod. Phys.* **C5**, 1073 (1992).
39. A. Billoire, E. Marinari and G. Parisi, *Phys. Lett. B* **162**, 160 (1985); R.D. Kenway, in: *Proc. XXII Int. Conf. on High Energy Physics (Leipzig, 1984)*, ed. A. Meyer and E. Wieczorek.
40. P. Bacilieri *et al.*, *Nucl. Phys. B* **317**, 509 (1989).
41. E. Marinari, *Nucl. Phys. B (Proc. Suppl.)* **9**, 209 (1989); F. Butler *et al.*, *Nucl. Phys. B (Proc. Suppl.)* **26**, 287 (1992).
42. E. Eichten, G. Hockney and H.B. Thacker, *Nucl. Phys. B (Proc. Suppl.)* **17**, 529 (1990).
43. S. Güsken *et al.*, *Nucl. Phys. B (Proc. Suppl.)* **17**, 362 (1990); *Phys. Lett. B* **227**, 266 (1989);

44. UKQCD Collaboration (C.R. Allton *et al.*), *Phys. Rev. D* **47**, 5128 (1993).
45. R. Sommer, *Nucl. Phys. B* **411**, 839 (1994).
46. K. Symanzik, in: *Mathematical problems in theoretical physics*, eds. R. Schrader *et al.*, Lecture Notes in Physics, Vol. 153 (Springer, New York, 1982); *Nucl. Phys. B* **226**, 187 (1983), and *ibid.*, 205.
47. M. Lüscher and P. Weisz, *Commun. Math. Phys.* **97**, 59 (1985); *E: Commun. Math. Phys.* **98** (1985) 433.
48. B. Sheikholeslami and R. Wohlert, *Nucl. Phys. B* **259**, 572 (1985).
49. G. Heatlie, C.T. Sachrajda, G. Martinelli, C. Pittori and G.C. Rossi, *Nucl. Phys. B* **352**, 266 (1991).
50. M. Lüscher, S. Sint, R. Sommer and P. Weisz, *Nucl. Phys. B* **478**, 365 (1996).
51. M. Lüscher and P. Weisz, *Nucl. Phys. B* **479**, 429 (1996).
52. M. Lüscher, S. Sint, R. Sommer, P. Weisz and U. Wolff, *Nucl. Phys. B* **491**, 323 (1997).
53. M. Lüscher, S. Sint, R. Sommer and H. Wittig, *Nucl. Phys. B* **491**, 344 (1997).
54. G.P. Lepage, *Nucl. Phys. B* (Proc. Suppl.) **26**, 45 (1992).
55. A.S. Kronfeld, *Nucl. Phys. B* (Proc. Suppl.) **30**, 445 (1993).
56. P.B. Mackenzie, *Nucl. Phys. B* (Proc. Suppl.) **30**, 35 (1993).
57. G.P. Lepage and P.B. Mackenzie, *Nucl. Phys. B* (Proc. Suppl.) **20**, 173 (1992); *Phys. Rev. D* **48**, 2250 (1992).
58. A.X. El-Khadra, A.S. Kronfeld and P.B. Mackenzie, *Phys. Rev. D* **55**, 3933 (1997).
59. Ph. Boucaud, C.L. Lin and O. Pène, *Phys. Rev. D* **40**, 1529 (1989).
60. E. Eichten and B.R. Hill, *Phys. Lett. B* **234**, 511 (1990).
61. E. Eichten and B.R. Hill, *Phys. Lett. B* **240**, 193 (1990).
62. A. Borrelli and C. Pittori, *Nucl. Phys. B* **385**, 502 (1992).
63. O.F. Hernández and B.R. Hill, *Phys. Lett. B* **289**, 417 (1992).
64. J.M. Flynn, O.F. Hernández and B.R. Hill, *Phys. Rev. D* **43**, 3709 (1991).
65. V. Giménez, *Nucl. Phys. B* **375**, 582 (1992).
66. V. Giménez, *Nucl. Phys. B* **401**, 116 (1993).
67. M. Ciuchini, E. Franco and V. Giménez, *Phys. Lett. B* **388**, 167 (1996).
68. G. Buchalla, *Phys. Lett. B* **395**, 364 (1997).
69. L. Maiani, G. Martinelli and C.T. Sachrajda, *Nucl. Phys. B* **368**, 281 (1992); G. Martinelli and C.T. Sachrajda, *Phys. Lett. B* **354**, 423 (1995).
70. B.A. Thacker and G.P. Lepage, *Phys. Rev. D* **43**, 196 (1991); G.P. Lepage, L. Magnea, C. Nakhleh, U. Magnea and K. Hornbostel, *Phys. Rev. D* **46**, 4052 (1992).
71. M. Bochicchio, L. Maiani, G. Martinelli, G. Rossi and M. Testa, *Nucl. Phys. B* **262**, 331 (1985).
72. L. Maiani and G. Martinelli, *Phys. Lett. B* **178**, 265 (1986).
73. B. Meyer and C. Smith, *Phys. Lett. B* **123**, 62 (1983).
74. G. Martinelli and Y. Zhang, *Phys. Lett. B* **123**, 433 (1983); *Phys. Lett. B* **125**, 77 (1983).
75. R. Groot, J. Hoek and J. Smit, *Nucl. Phys. B* **237**, 111 (1984).
76. E. Gabrielli, G. Martinelli, C. Pittori, G. Heatlie and C.T. Sachrajda, *Nucl. Phys. B* **362**, 475 (1991).
77. A. Borelli, C. Pittori, R. Frezzotti and E. Gabrielli, *Nucl. Phys. B* **409**, 382 (1993).
78. G. Parisi, in: Proc. XX Int. Conf. on High Energy Physics (Madison, Wisconsin, 1980), ed. L. Durand and L.G. Pondrom (American Institute of Physics, New York, 1981).
79. G. Martinelli, C. Pittori, C.T. Sachrajda and A. Vladikas, *Phys. Lett. B* **331**, 241 (1993); erratum: *Phys. Lett. B* **317**, 660 (1993).
80. M.L. Paciello, S. Petrarca, B. Taglienti and A. Vladikas, *Phys. Lett. B* **341**, 187 (1994).
81. UKQCD Collaboration (D.S. Henty *et al.*), *Phys. Rev. D* **51**, 5323 (1995).
82. G. Martinelli, C. Pittori, C.T. Sachrajda, M. Testa and A. Vladikas, *Nucl. Phys. B*

- (Proc. Suppl.) **42**, 428 (1995); *Nucl. Phys. B* **445**, 81 (1995).
83. M. Göckeler *et al.*, *Nucl. Phys. B* (Proc. Suppl.) **47**, 493 (1996).
  84. A. Donini *et al.*, *Nucl. Phys. B* (Proc. Suppl.) **47**, 489 (1996).
  85. A. Donini *et al.*, *Phys. Lett. B* **360**, 83 (1995);
  86. M. Alford, W. Dimm, G.P. Lepage, G. Hockney and P.B. Mackenzie, *Nucl. Phys. B* (Proc. Suppl.) **42**, 787 (1995); *Phys. Lett. B* **361**, 87 (1995).
  87. M. Alford, T. Klassen and G.P. Lepage, *Nucl. Phys. B* (Proc. Suppl.) **47**, 409 (1996); *Improving Lattice Quark Actions*, FSU-SCRI-96C-134, [hep-lat/9611010](#).
  88. P. Hasenfratz and F. Niedermayer, *Nucl. Phys. B* **414**, 785 (1994); F. Falcioni, P. Hasenfratz, F. Niedermayer and A. Papa, *Nucl. Phys. B* **454**, 638 (1995).
  89. T. DeGrand, A. Hasenfratz, P. Hasenfratz and F. Niedermayer, *Nucl. Phys. B* **454**, 587 (1995); *ibid.* p.615; *Phys. Lett. B* **365**, 233 (1996); M. Blatter and F. Niedermayer, *Nucl. Phys. B* **482**, 286 (1996).
  90. W. Bietenholz and U.J. Wiese, *Nucl. Phys. B* (Proc. Suppl.) **34**, 516 (1994); *Nucl. Phys. B* **464**, 319 (1996); W. Bietenholz, E. Focht and U.J. Wiese, *Nucl. Phys. B* **436**, 385 (1995).
  91. M. Lüscher, *Commun. Math. Phys.* **104**, 177 (1986).
  92. M. Fukugita *et al.*, *Phys. Lett. B* **294**, 380 (1992).
  93. S. Aoki *et al.*, *Nucl. Phys. B* (Proc. Suppl.) **34**, 363 (1994).
  94. Ph. Boucaud, O. Pène, V.J. Hill, C.T. Sachrajda and G. Martinelli, *Phys. Lett. B* **220**, 219 (1989).
  95. M. Neubert, *Phys. Rev. D* **46**, 1076 (1992).
  96. X. Ji and M.J. Musolf, *Phys. Lett. B* **257**, 409 (1991).
  97. D.J. Broadhurst and A.G. Grozin, *Phys. Lett. B* **274**, 421 (1992).
  98. C. Alexandrou *et al.*, *Nucl. Phys. B* **414**, 815 (1994).
  99. C.W. Bernard, J.N. Labrenz and A. Soni, *Phys. Rev. D* **49**, 2536 (1994).
  100. UKQCD Collaboration (A.K. Ewing *et al.*), *Phys. Rev. D* **54**, 3526 (1996).
  101. UKQCD Collaboration (R.M. Baxter *et al.*), *Phys. Rev. D* **49**, 1594 (1994).
  102. C. Alexandrou *et al.*, *Z. Phys. C* **62**, 659 (1994).
  103. T. Draper and C. McNeile, *Nucl. Phys. B* (Proc. Suppl.) **47**, 429 (1996).
  104. A. Ali Khan *et al.*, *Nucl. Phys. B* (Proc. Suppl.) **47**, 425 (1996).
  105. S. Collins *et al.*, *Nucl. Phys. B* (Proc. Suppl.) **47**, 451 (1996).
  106. S. Collins *et al.*, *Phys. Rev. D* **55**, 1630 (1997).
  107. A. Ali Khan and T. Bhattacharya, *Nucl. Phys. B* (Proc. Suppl.) **53**, 368 (1997).
  108. A. Ali Khan *et al.*, *Heavy-light mesons with quenched lattice NRQCD: results on decay constants*, OHSTPY-HEP-T-97-006, [hep-lat/9704008](#).
  109. A. Abada *et al.*, *Nucl. Phys. B* **376**, 172 (1992).
  110. MILC Collaboration (C. Bernard *et al.*), presented at LAFEX International School on High Energy Physics, Rio de Janeiro, Brazil, 20–22 Feb 1995, [hep-ph/9503336](#).
  111. MILC Collaboration (C. Bernard *et al.*), *Nucl. Phys. B* (Proc. Suppl.) **42**, 388 (1995); *Nucl. Phys. B* (Proc. Suppl.) **47**, 459 (1996).
  112. MILC Collaboration (C. Bernard *et al.*), *Nucl. Phys. B* (Proc. Suppl.) **53**, 358 (1997).
  113. MILC Collaboration, private communication by C. Bernard.
  114. JLQCD Collaboration (S. Aoki *et al.*), *Nucl. Phys. B* (Proc. Suppl.) **47**, 433 (1996).
  115. JLQCD Collaboration (S. Aoki *et al.*), *Nucl. Phys. B* (Proc. Suppl.) **53**, 355 (1997).
  116. T. Bhattacharya and R. Gupta, *Phys. Rev. D* **54**, 1155 (1996).
  117. R. Gupta and T. Bhattacharya, *Nucl. Phys. B* (Proc. Suppl.) **473**, 473 (1996).
  118. C. Alexandrou *et al.*, *Phys. Lett. B* **256**, 60 (1991).
  119. APE Collaboration (C.R. Allton *et al.*), *Nucl. Phys. B* (Proc. Suppl.) **34**, 456 (1994), and private communication by C.R. Allton, 1996.
  120. C.R. Allton *et al.*, ROME prep. 97/1164, [hep-lat/9703002](#).

121. K.M. Bitar *et al.*, *Phys. Rev. D* **48**, 370 (1993).
122. K.M. Bitar *et al.*, *Phys. Rev. D* **49**, 3546 (1994).
123. C. Alexandrou *et al.*, *Nucl. Phys. B* **374**, 263 (1992).
124. M.B. Gavela *et al.*, *Nucl. Phys. B* **206**, 113 (1988).
125. T.A. DeGrand and R.D. Loft, *Phys. Rev. D* **38**, 954 (1988).
126. C. Bernard, T. Draper, G. Hockney and A. Soni, *Phys. Rev. D* **38**, 3540 (1988).
127. APE Collaboration (C.R. Allton *et al.*), *Nucl. Phys. B (Proc. Suppl.)* **42**, 385 (1995).
128. A. Duncan *et al.*, *Phys. Rev. D* **51**, 5101 (1995).
129. APE Collaboration (C.R. Allton *et al.*), *Phys. Lett. B* **326**, 295 (1994).
130. T. Draper and C. McNeile, *Nucl. Phys. B (Proc. Suppl.)* **34**, 453 (1994).
131. T. Draper, C. McNeile and C. Nenkov, *Nucl. Phys. B (Proc. Suppl.)* **42**, 325 (1995).
132. S. Hashimoto, *Phys. Rev. D* **50**, 4639 (1994).
133. APE Collaboration (C.R. Allton *et al.*), *Nucl. Phys. B* **413**, 461 (1994).
134. S. Hashimoto and Y. Saeki, *Mod. Phys. Lett. A* **7**, 387 (1992).
135. C. Allton *et al.*, *Nucl. Phys. B* **349**, 598 (1991).
136. G.M. de Divitiis, R. Frezzotti, M. Masetti and R. Petronzio, *Phys. Lett. B* **382**, 393 (1996), and *ibid.*, 398.
137. MILC Collaboration (C. Bernard *et al.*), *Nucl. Phys. B (Proc. Suppl.)* **53**, 374 (1997).
138. B. Berg and A. Billoire, *Nucl. Phys. B* **221**, 109 (1983); G.C. Fox, R. Gupta, O. Martin and S. Otto, *Nucl. Phys. B* **205**, 188 (1982); M. Lüscher and U. Wolff, *Nucl. Phys. B* **339**, 222 (1990); A.S. Kronfeld, *Nucl. Phys. B (Proc. Suppl.)* **17**, 313 (1990).
139. C. Allton, *Nucl. Phys. B* **437**, 641 (1995).
140. M. Neubert, *Phys. Rev. D* **45**, 2451 (1992).
141. V. Eletskii and E. Shuryak, *Phys. Lett. B* **276**, 191 (1992).
142. E. Bagan, P. Ball, V.M. Braun and H.G. Dosch, *Phys. Lett. B* **278**, 457 (1992).
143. C.A. Dominguez, talk presented at III Workshop on Tau-Charm Factory, Marbella, Spain, June 1993, [hep-ph/9309160](#).
144. S. Narison, *Z. Phys. C* **55**, 671 (1992).
145. S. Narison, *Phys. Lett. B* **308**, 365 (1993).
146. S. Narison, *Phys. Lett. B* **322**, 247 (1994).
147. S. Narison, *Phys. Lett. B* **352**, 122 (1995).
148. P. Ball, *Phys. Lett. B* **421**, 593 (1994).
149. Particle Data Group (R.M. Barnett *et al.*), *Phys. Rev. D* **54**, 1 (1996).
150. J.D. Richman, Invited talk at 28th International Conference on High-energy Physics (ICHEP 96), Warsaw, Poland, 25–31 July 1996, [hep-ex/9701014](#).
151. E653 Collaboration (K. Kodama *et al.*), *Phys. Lett. B* **382**, 299 (1996).
152. WA75 Collaboration (S. Aoki *et al.*), *Prog. Theor. Phys.* **89**, 131 (1993).
153. CLEO Collaboration (D. Gibaut *et al.*), preprint CLEO-CONF 95-22, submitted to the European Physical Society Conference, Brussels, Belgium (1995), [eps-0184](#).
154. BES Collaboration (J.Z. Bai *et al.*), *Phys. Rev. Lett.* **74**, 4599 (1995).
155. L3 Collaboration (M. Acciarri *et al.*), preprint CERN-PPE-97-012, submitted to *Phys. Lett. B*.
156. S. Capstick and S. Godfrey, *Phys. Rev. D* **41**, 2856 (1990).
157. R.J. Oakes, *Phys. Rev. Lett.* **73**, 381 (1994).
158. D.S. Hwang and G.-H. Kim, *Phys. Rev. D* **53**, 3659 (1996).
159. D.S. Hwang and G.-H. Kim, *Phys. Lett. B* **367**, 353 (1996).
160. C.G. Boyd, B. Grinstein and R.F. Lebed, *Phys. Rev. Lett.* **74**, 4603 (1995).
161. A. Buras, M. Jamin and P.H. Weisz, *Nucl. Phys. B* **347**, 491 (1990).
162. V. Giménez and G. Martinelli, *Phys. Lett. B* **398**, 135 (1997).
163. J. Christensen, T. Draper and C. McNeile, UK-96-11, [hep-lat/9610026](#).
164. A. Soni, *Nucl. Phys. B (Proc. Suppl.)* **47**, 43 (1996).

165. C. Bernard, T. Blum and A. Soni, *Nucl. Phys. B* (Proc. Suppl.) **53**, 382 (1997).
166. S. Narison and A.A. Pivovarov, *Phys. Lett. B* **327**, 341 (1994).
167. A. Pich, *Phys. Lett. B* **206**, 322 (1988).
168. L. Wolfenstein, *Phys. Rev. Lett.* **51**, 1945 (1983).
169. A.J. Buras, M.E. Lautenbacher and G. Ostermaier, *Phys. Rev. D* **50**, 3433 (1994).
170. L. Gibbons, Invited talk at 28th International Conference on High-energy Physics (ICHEP 96), Warsaw, Poland, 25-31 Jul 1996, [hep-ex/9704017](#).
171. R. Tipton, presented at the 28th International Conference on High Energy Physics, 25-31 July, Warsaw, Poland.
172. C. Zeitz, invited talk presented at BEAUTY 96, 17-21 June 1996, Rome, Italy.
173. ALEPH Collaboration, presented at the 28th International Conference on High Energy Physics, 25-31 July, Warsaw, Poland, ICHEP96 PA08-020.
174. A. Czarnecki, *Phys. Rev. Lett.* **76**, 4124 (1996).
175. A. Ali and D. London, *Z. Phys. C* **65**, 431 (1995).
176. A. Ali and D. London, *Nucl. Phys. B* (Proc. Suppl.) **54A**, 297 (1997).
177. T. Inami and C.S. Lim, *Progr. Theor. Phys.* **65**, 297 (1981); *ibid.* p. 1772.
178. A.J. Buras, *Phys. Rev. Lett.* **46**, 1354 (1981).
179. S. Herrlich and U. Nierste, *Phys. Rev. D* **52**, 6505 (1995).
180. S. Herrlich and U. Nierste, *Nucl. Phys. B* **476**, 27 (1996).
181. S. Herrlich, presented at the 28th International Conference on High Energy Physics, 25-31 July, Warsaw, Poland, [hep-ph/9609376](#).
182. W.A. Bardeen, A.J. Buras and J.-M. Gérard, *Phys. Lett. B* **211**, 343 (1988).
183. J.-M. Gérard, *Acta Phys. Pol. B* **21**, 257 (1990).
184. J. Bijnens and J. Prades, *Nucl. Phys. B* **444**, 523 (1995).
185. S. Sharpe, *Nucl. Phys. B* (Proc. Suppl.) **34**, 403 (1994).
186. M. Crisafulli *et al.*, *Phys. Lett. B* **369**, 325 (1996).
187. JLQCD Collaboration (S. Aoki *et al.*), *Nucl. Phys. B* (Proc. Suppl.) **47**, 465 (1996).
188. N. Ishizuka *et al.*, *Phys. Rev. Lett.* **71**, 24 (1993).
189. S. Sharpe, *Nucl. Phys. B* (Proc. Suppl.) **53**, 181 (1997).
190. JLQCD Collaboration, *Nucl. Phys. B* (Proc. Suppl.) **53**, 341 (1997).
191. JLQCD Collaboration, *Nucl. Phys. B* (Proc. Suppl.) **53**, 349 (1997).
192. A. Donini *et al.*, *Nucl. Phys. B* (Proc. Suppl.) **53**, 883 (1997).
193. G. Kilcup, D. Pekurovsky, L. Venkataraman, *Nucl. Phys. B* (Proc. Suppl.) **53**, 345 (1997).
194. A.J. Buras, *Nucl. Instrum. Meth. A* **368**, 1 (1995).
195. UKQCD Collaboration (S.P. Booth *et al.*), *Phys. Lett. B* **294**, 385 (1992).
196. G.S. Bali and K. Schilling, *Phys. Rev. D* **47**, 661 (1993).
197. M. Lüscher, R. Sommer, P. Weisz and U. Wolff, *Nucl. Phys. B* **413**, 481 (1994).
198. UKQCD Collaboration (H. Wittig), *Nucl. Phys. B* (Proc. Suppl.) **42**, 288 (1995), [hep-lat/9411075](#); private notes, 1996.
199. UKQCD Collaboration (C.R. Allton *et al.*), *Nucl. Phys. B* **407**, 1993 (331).
200. C. Michael and S.J. Perantonis, *Nucl. Phys. B* **347**, 854 (1990).
201. K.D. Born *et al.*, *Nucl. Phys. B* (Proc. Suppl.) **20**, 394 (1991).
202. SESAM Collaboration (U. Glässner *et al.*), *Phys. Lett. B* **383**, 98 (1996).
203. A.X. El-Khadra, G. Hockney, A.S. Kronfeld, P.B. Mackenzie, *Phys. Rev. Lett.* **69**, 729 (1992).
204. JLQCD Collaboration (S. Aoki *et al.*), *Nucl. Phys. B* (Proc. Suppl.) **47**, 354 (1996).
205. F. Butler, H. Chen, J. Sexton, A. Vaccarino and D. Weingarten, *Nucl. Phys. B* **421**, 217 (1994).
206. F. Butler, H. Chen, J. Sexton, A. Vaccarino and D. Weingarten, *Nucl. Phys. B* **430**, 179 (1994).

207. S. Cabasino *et al.*, *Phys. Lett. B* **258**, 195 (1991).
208. T. Bhattacharya, R. Gupta, G. Kilcup and S. Sharpe, *Phys. Rev. D* **53**, 6486 (1996).
209. QCDPAX Collaboration (Y. Iwasaki *et al.*), *Phys. Rev. D* **53**, 6443 (1996).
210. M. Göckeler *et al.*, *Phys. Lett. B* **391**, 388 (1997).
211. C.R. Allton, V. Giménez, L. Giusti and F. Rapuano, *Nucl. Phys. B* **489**, 427 (1997).
212. UKQCD Collaboration (C.R. Allton *et al.*), *Phys. Rev. D* **49**, 1994 (474).
213. UKQCD Collaboration (C. Michael and H.P. Shanahan), *Nucl. Phys. B* (Proc. Suppl.) **47**, 1996 (337).
214. UKQCD Collaboration (H.P. Shanahan *et al.*), *Phys. Rev. D* **55**, 1997 (1548).
215. UKQCD Collaboration (R.D. Kenway), presented at *Lattice QCD on Parallel Computers*, March 1997, Tsukuba, Japan; UKQCD Collaboration, in preparation.